

AD-A196 534

③

AD _____

NOT FILE COPY

**Biochemical Changes in Human Erythrocyte Membranes
During Prolonged Cold Storage Under Bank Conditions**

Final Report

Vann Bennett, Ph.D.

May 1, 1988

Supported by

U.S. ARMY MEDICAL RESEARCH AND DEVELOPMENT COMMAND
Fort Detrick, Frederick, Maryland 21701-5012

Contract No. DAMD17-83-C-3209

Johns Hopkins University
School of Medicine
725 N. Wolfe Street
Baltimore, MD 21205

DTIC
ELECTE
S JUN 14 1988 D
E

DOD DISTRIBUTION STATEMENT

Approved for public release; distribution unlimited

The findings in this report are not to be construed as an official Department of the Army position unless so designated by other authorized documents.

REPORT DOCUMENTATION PAGE

Form Approved
OMB No. 0704-0188

1a. REPORT SECURITY CLASSIFICATION Unclassified			1b. RESTRICTIVE MARKINGS		
2a. SECURITY CLASSIFICATION AUTHORITY			3. DISTRIBUTION/AVAILABILITY OF REPORT Approved for public release; distribution unlimited		
2b. DECLASSIFICATION/DOWNGRADING SCHEDULE			4. PERFORMING ORGANIZATION REPORT NUMBER(S)		
6a. NAME OF PERFORMING ORGANIZATION Johns Hopkins University School of Medicine			6b. OFFICE SYMBOL (if applicable)		7a. NAME OF MONITORING ORGANIZATION
6c. ADDRESS (City, State, and ZIP Code) 725 N. Wolfe Street Baltimore, MD 21205			7b. ADDRESS (City, State, and ZIP Code)		
8a. NAME OF FUNDING/SPONSORING ORGANIZATION U.S. Army Medical Research & Development Command		8b. OFFICE SYMBOL (if applicable)		9. PROCUREMENT INSTRUMENT IDENTIFICATION NUMBER Contract No. DAMD17-83-C-3209	
8c. ADDRESS (City, State, and ZIP Code) Fort Detrick Frederick, Maryland 21701-5012			10. SOURCE OF FUNDING NUMBERS		
			PROGRAM ELEMENT NO. 62772A	PROJECT NO. 3S16 2772A874	TASK NO. AD
			WORK UNIT ACCESSION NO. 158		
11. TITLE (Include Security Classification) Biochemical Changes in Human Erythrocyte Membranes During Prolonged Cold Storage Under Blood Bank Conditions					
12. PERSONAL AUTHOR(S) Vann Bennett, Ph.D.					
13a. TYPE OF REPORT Final Report		13b. TIME COVERED FROM 8/1/83 TO 7/31/84		14. DATE OF REPORT (Year, Month, Day) 1988 May 1	
15. PAGE COUNT 3					
16. SUPPLEMENTARY NOTATION					
17. COSATI CODES			18. SUBJECT TERMS (Continue on reverse if necessary and identify by block number)		
FIELD	GROUP	SUB-GROUP	Erythrocytes, Cold Storage, CPD-Adenine, Phosphorylation, Spectrin, Ankyrin		
06	01				
06	05				
19. ABSTRACT (Continue on reverse if necessary and identify by block number)					
<p>Initial goals of the research on blood aged under blood bank conditions were to evaluate the possible role of elevation in intracellular calcium in mediating damage to the membrane skeleton of these cells. The possible elevation of intracellular calcium in aged red cells was evaluated by determining the extent of degradation of ankyrin, a protein known to be extremely sensitive to calcium-mediated proteolysis. Blood aged up to 8 weeks showed no increase in degradation of ankyrin, as determined by immunoblot analysis using affinity purified antibody against human erythrocyte ankyrin. These results suggested that the aged erythrocyte does not experience elevations of free intracellular calcium above 1-10uM, which is the range of concentrations where proteolysis of ankyrin occurs. The initial hypothesis concerning a role for calcium in mediating damage to stored erythrocytes thus was most likely incorrect.</p> <p>Other aspects of membrane skeletal proteins that were examined in erythrocytes from aged blood included association of ankyrin with ankyrin-depleted inside-out vesicles, association</p> <p style="text-align: right;">(Continued)</p>					
20. DISTRIBUTION/AVAILABILITY OF ABSTRACT <input type="checkbox"/> UNCLASSIFIED/UNLIMITED <input checked="" type="checkbox"/> SAME AS RPT. <input type="checkbox"/> DTIC USERS			21. ABSTRACT SECURITY CLASSIFICATION Unclassified		
22a. NAME OF RESPONSIBLE INDIVIDUAL Mrs. Virginia Miller			22b. TELEPHONE (Include Area Code) 301/663-7325		22c. OFFICE SYMBOL SGRD-RMI-S

19. Abstract(Continued)

of spectrin with spectrin-depleted inside-out vesicles, and possible degradation of the anion transporter as determined by immunoblot analysis. In all cases, erythrocytes from blood aged 7-9 weeks were indistinguishable from those from freshly drawn blood or blood aged 1-2 weeks.

Other experiments directed towards understanding normal erythrocytes were more successful. Four new proteins were purified and characterized from human erythrocytes: myosin, clathrin, clathrin uncoating protein, and a major calmodulin-binding protein associated with the membrane skeleton. In another study also partially funded by the contract the anion transporter was identified as a possible receptor for the malaria parasite *P. falciparum*.

Studies funded in part by the contract have resulted in the following publications:

1. Fowler, V., Davis, J., and Bennett, V. Human erythrocyte myosin: Identification and purification. (1985) J. Cell Biology 100, 47-55.
2. Okoye, V., and Bennett, V. *Plasmodium falciparum* Malaria: Band 3 as a possible receptor during invasion of human erythrocytes. (1985) Science 227, 169-171.
3. Davis, J. and Bennett, V. Human erythrocyte clathrin and clathrin-uncoating protein. (1985) J. Biol. Chem. 260, 14850-14856.
4. Gardner, K. and Bennett, V. A new erythrocyte membrane-associated protein with calmodulin-binding activity. (1986) J. Biol. Chem. 261, 1339-1348.

DISTRIBUTION LIST

4 copies

Commander
 Letterman Army Institute of
 Research (LAIR), Bldg. 1110
 ATTN: SGRD-ULZ-RC
 Presidio of San Francisco, CA 94129-6815

1 copy

Commander
 US Army Medical Research and Development Command
 ATTN: SGRD-RMI-S
 Fort Detrick, Frederick, Maryland 21701-5012

2 copies

Defense Technical Information Center (DTIC)
 ATTN: DTIC-DDAC
 Cameron Station
 Alexandria, VA 22304-6145

1 copy

Dean
 School of Medicine
 Uniformed Services University of the
 Health Sciences
 4301 Jones Bridge Road
 Bethesda, MD 20814-4799

1 copy

Commandant
 Academy of Health Sciences, US Army
 ATTN: AHS-CDM
 Fort Sam Houston, TX 78234-6100



Accession For	
NTIS GRA&I	<input checked="" type="checkbox"/>
DTIC TAB	<input type="checkbox"/>
Unannounced	<input type="checkbox"/>
Justification	
By _____	
Distribution/	
Availability Codes	
Dist	Avail and/or Special
A-1	

Human Erythrocyte Myosin: Identification and Purification

VELIA M. FOWLER, JONATHAN Q. DAVIS, and VANN BENNETT

Department of Cell Biology and Anatomy, The Johns Hopkins University School of Medicine, Baltimore, Maryland 21205. Dr. Fowler's present address is Department of Anatomy, Harvard Medical School, Boston, Massachusetts 02115.

ABSTRACT Human erythrocytes contain an M_r 200,000 polypeptide that cross-reacts specifically with affinity-purified antibodies to the M_r 200,000 heavy chain of human platelet myosin. Immunofluorescence staining of formaldehyde-fixed erythrocytes demonstrated that the immunoreactive myosin polypeptide is present in all cells and is localized in a punctate pattern throughout the cell. Between 20–40% of the immunoreactive myosin polypeptide remained associated with the membranes after hemolysis and preparation of ghosts, suggesting that it may be bound to the membrane cytoskeleton as well as being present in the cytosol. The immunoreactive myosin polypeptide was purified from the hemolysate to ~85% purity by DEAE-cellulose chromatography followed by gel filtration on Sephacryl S-400. The purified protein is an authentic vertebrate myosin with two globular heads at the end of a rod-like tail ~150-nm long, as visualized by rotary shadowing of individual molecules, and with two light chains (M_r 25,000 and 19,500) in association with the M_r 200,000 heavy chain. Peptide maps of the M_r 200,000 heavy chains of erythrocyte and platelet myosin were seen to be nearly identical, but the proteins are distinct since the platelet myosin light chains migrate differently on SDS gels (M_r 20,000 and 17,000). The erythrocyte myosin formed bipolar filaments 0.3–0.4- μ m long at physiological salt concentrations and exhibited a characteristic pattern of myosin ATPase activities with EDTA, Ca^{++} , and Mg^{++} -ATPase activities in 0.5 M KCl of 0.38, 0.48, and <0.01 $\mu\text{mol/min per mg}$. The Mg^{++} -ATPase activity of erythrocyte myosin in 0.06 M KCl (<0.01 $\mu\text{mol/min per mg}$) was not stimulated by the addition of rabbit muscle F-actin. The erythrocyte myosin was present in about 6,000 copies per cell, in a ratio of 80 actin monomers for every myosin molecule, which is an amount comparable to actin/myosin ratios in other nonmuscle cells. The erythrocyte myosin could function together with tropomyosin on the erythrocyte membrane (Fowler, V. M., and V. Bennett, 1984, *J. Biol. Chem.*, 259:5978–5989) in an actomyosin contractile apparatus responsible for ATP-dependent changes in erythrocyte shape.

Underlying the plasma membrane of eucaryotic cells is a cytoskeletal actin filament network that is believed to play a structural role in determining cell architecture as well as a dynamic role in generating membrane movements. The molecular organization of this membrane cytoskeleton is best understood in the human erythrocyte, a cell with a unique biconcave disk shape, remarkable deformability properties, and no intracellular membranes or organelles. The available evidence indicates that the erythrocyte membrane cytoskeleton is constructed of many short actin filaments (~12–20 monomers long) (26, 35) that are cross-linked into an anastomosing network in the plane of the membrane by long, flexible spectrin molecules in association with an M_r ~80,000

helper protein, band 4.1. The entire cytoskeletal ensemble is attached to the cytoplasmic surface of the membrane via the specific association of spectrin with ankyrin, an M_r ~210,000 protein that is itself tightly bound to the cytoplasmic domain of band 3, the anion channel, and major integral membrane protein (for recent reviews, see references 5, 7). The recent isolation of spectrin- and ankyrin-like proteins from nonerythrocyte cells and tissues and their localization on the plasma membrane (4, 10) encourage the view that the organization of the erythrocyte membrane cytoskeleton could indeed be representative of the plasma membrane cytoskeleton of nucleated cells, at least in certain regions. However, as currently depicted, this model is an essentially static one and

does not account for the plasma membrane movements of nucleated cells (e.g., membrane ruffling, filopodial extension and retraction, and endo- and exocytosis), nor for dynamic ATP-dependent discocyte-echinocyte shape transformations of erythrocytes (22, 24, 34, 37).

We describe here the identification and purification of myosin from human erythrocytes. The erythrocyte myosin was found to be present with respect to the erythrocyte actin in a ratio of about 80 actin monomers to 1 myosin molecule, an amount comparable to actin/myosin ratios in other non-muscle cells. In addition, we have recently identified a non-muscle form of tropomyosin on the erythrocyte membrane that is present in sufficient quantities to almost completely coat all of the short actin filaments in the membrane cytoskeleton (14). This suggests that the erythrocyte myosin is not simply a relic from a previous developmental stage of the cell and supports the hypothesis that a membrane-associated actomyosin contractile apparatus could be responsible for ATP-dependent changes in erythrocyte shape and deformability.

MATERIALS AND METHODS

Production and Purification of Antibodies: Myosin was purified from outdated human platelets as described by Pollard et al. (28) and was stored at 4°C as a slurry in 60% saturated ammonium sulfate. Three New Zealand white rabbits were injected subcutaneously at multiple sites on the back and sides with 100–150 µg each of native myosin in complete Freund's adjuvant, followed by booster injections with antigen in incomplete Freund's adjuvant after 3 wk, and then at 1–2-mo intervals thereafter. Titer was monitored by the immunoblot method (see below) and was high after the third injection. Immune serum was diluted with 1 vol of 150 mM NaCl, 10 mM sodium phosphate, 1 mM EDTA, 1 mM Na₂S₂O₃, 0.2% (vol/vol) Triton X-100, heated to 60°C in the presence of 200 µg/ml phenylmethylsulfonyl fluoride to minimize protease activity, and stored at –20°C. Antibody against platelet myosin was isolated by affinity chromatography with myosin coupled to cyanogen bromide-activated Sepharose (Cl) 4B (Pharmacia Fine Chemicals, Piscataway, NJ) (0.7 mg of myosin/ml of agarose). 10–20 ml of immune serum was applied to a 3.5-ml column, the column was washed, and antibody was eluted as described previously (14). Peak fractions (based on A₂₈₀) were pooled, concentrated three- to fourfold by dialysis into 150 mM NaCl, 10 mM sodium phosphate, 1 mM Na EDTA, 0.02% Na₂S₂O₃, pH 7.5, 50% glycerol at 4°C, and stored at –20°C. Yields of purified antibody ranged from 0.03 to 0.10 mg (based on E₂₈₀ = 14) per milliliter of diluted serum, depending on the rabbit. Although the antibodies were isolated by affinity chromatography with native platelet myosin, they were specific for the heavy chain and did not label the light chains in immunoblotting assays. Ig was isolated from preimmune serum by affinity chromatography on Protein A-Sepharose (14). Affinity-purified antibodies to human erythrocyte spectrin were a gift from Dr. Peter C. Agre (Department of Medicine, The Johns Hopkins University School of Medicine).

Preparation of Hemolysate, Membranes, and Purified Proteins: Erythrocytes were isolated from freshly drawn human blood anticoagulated with acid/citrate/dextrose as described (6). Cells were lysed in 10–15 vol of ice-cold 7.5 mM sodium phosphate, 1 mM EDTA, 2 mM dithiothreitol (DTT), 20 µg/ml of phenylmethylsulfonyl fluoride, pH 7.5, and the membranes were pelleted by centrifugation as described (6); this supernatant is referred to as the hemolysate. Membranes were prepared by three more washes in the lysis buffer (6). Ankyrin and spectrin were purified from membranes as described (6), and the M_r 200,000 immunoreactive myosin polypeptide from the hemolysate as described in the text and the legend to Fig. 3. Protein concentrations for the purified proteins were determined spectrophotometrically from the absorbance at 280 nm (after correction for light scattering at 320 nm) based on an E₂₈₀ value of 10 for spectrin and ankyrin, and 5.9 for myosin (28).

Electrophoresis and Immunoblotting Procedures: Electrophoresis was performed on 5–15% acrylamide linear gradient SDS gels in the presence of 4 M urea, with a 5% stacking gel containing 2 M urea, and with sample preparation and molecular weight standards as described previously (14). Electrophoretic transfer of polypeptides from the SDS gels to nitrocellulose paper was performed as described previously (14) except that gels were trans-

ferred for 6 h at 500–700 mA current at 15°C. Nitrocellulose gel transfers were labeled overnight (12–18 h) at 4°C with 2–4 µg/ml of affinity-purified antibodies to human platelet myosin, and processed for antibody detection with ¹²⁵I-Protein A (2 × 10⁶ cpm/ml) as described (14).

We quantitated the amount of the M_r 200,000 immunoreactive myosin polypeptide in a sample by staining the protein on the nitrocellulose transfers with 0.2% ponceau S in 3% trichloroacetic acid (10 min at room temperature followed by two washes in distilled water), cutting out the appropriate region of the nitrocellulose, and counting the ¹²⁵I-Protein A-labeled band in the gamma counter. The actual micrograms of the immunoreactive myosin polypeptide were computed from a standard curve prepared from immunoblots of known amounts of purified erythrocyte myosin that were electrophoresed on SDS gels and transferred to nitrocellulose in parallel with the unknowns. The standard curve was linear from ~0.02 to at least 0.25 µg of protein, and duplicate samples were reproducible ± 5%. The concentration of the purified erythrocyte myosin for the standard curve was based on the A₂₈₀, assuming E₂₈₀ = 5.9 (28), and corrected for the purity of the preparation (~85%; see Results) by multiplying by a factor of 1.2.

Immunofluorescence of Erythrocytes: Erythrocytes (isolated as described above) were fixed in suspension (10% [vol/vol] in 3% (wt/vol) paraformaldehyde in PBS (150 mM NaCl, 10 mM sodium phosphate, pH 7.5) for 15 min at room temperature, and then allowed to settle onto poly-L-lysine-coated coverslips (No. 2) for an additional 5 min at room temperature. Coverslips were washed three times in PBS, incubated 30 min at room temperature in 50 mM NH₄Cl in PBS, and then washed three times in PBS. Cells on coverslips were permeabilized by a 30-s incubation in acetone at –20°C, transferred immediately to PBS containing 0.2% gelatin (PBS/gelatin), and then washed two times in PBS/gelatin. Coverslips were placed over 50-µl drops of affinity-purified antibodies or preimmune Ig (10 µg/ml in PBS/gelatin) and incubated for 30 min at room temperature in a humid chamber. After four washes in PBS/gelatin they were incubated for 20 min at room temperature with tetramethyl rhodamine isothiocyanate goat anti-rabbit IgG (Miles Laboratories, Elkhart, IN) (1/400 dilution in PBS/gelatin). Following two washes in PBS/gelatin and two washes in PBS, coverslips were mounted on slides in 50% glycerol, 50% PBS and examined in a Zeiss microscope equipped with epifluorescence optics. Micrographs were taken with Kodak Tri-X pan film, ASA 800.

Antimyosin staining of erythrocytes was only obtained with the formaldehyde fixation, acetone postfixation/permeabilization protocol described above. Formaldehyde fixation followed by permeabilization with 0.1% Triton X-100 resulted in extraction of the phase-dense cytoplasmic contents of the cells and completely eliminated the antimyosin staining. Also, no specific staining was visible with acetone treatment alone in the absence of formaldehyde fixation. The antispectrin staining was identical regardless of the fixation/permeabilization protocol.

Electron Microscopy: For rotary shadowing, purified erythrocyte myosin in 0.5 M KCl was dialyzed at a concentration of 30 µg/ml against 100 mM ammonium formate, 30% (vol/vol) glycerol, pH 7.0, sprayed onto freshly cleaved mica, dried under vacuum at room temperature, and rotary shadowed at an angle of 1–10° with platinum followed by carbon (36). For negative staining, purified myosin in 0.5 M KCl was dialyzed at a concentration of 200 µg/ml against 50 mM KCl, 2 mM MgCl₂, 10 mM PIPES, pH 7.0, 4°C, to form filaments. After dilution and application to Formvar- and carbon-coated grids, the myosin was negatively stained with 1% uranyl acetate. Rotary shadowed and negatively stained samples were photographed using a Zeiss microscope operating at 80 kV.

RESULTS

Identification of Myosin in Human Erythrocytes

Previous attempts to identify myosin in human erythrocytes have been frustrated by the similarity in molecular weight of the myosin heavy chain (M_r 200,000) to the major membrane-associated cytoskeletal proteins spectrin (M_r of band 2 ~220,000) and ankyrin (M_r ~210,000), and by high levels of ATP hydrolysis resulting from membrane-associated ion pumps and coupled kinase-phosphatase activities in whole-cell lysates, membranes, and membrane extracts. To circumvent these problems, we prepared antibodies to platelet myosin to use as a specific probe in assaying for the presence of myosin in erythrocytes. Fig. 1 shows that affinity-purified antibodies to the M_r 200,000 heavy chain of human platelet myosin cross-reacted with an M_r 200,000 polypeptide in

¹ Abbreviation used in this paper: DTT, dithiothreitol.

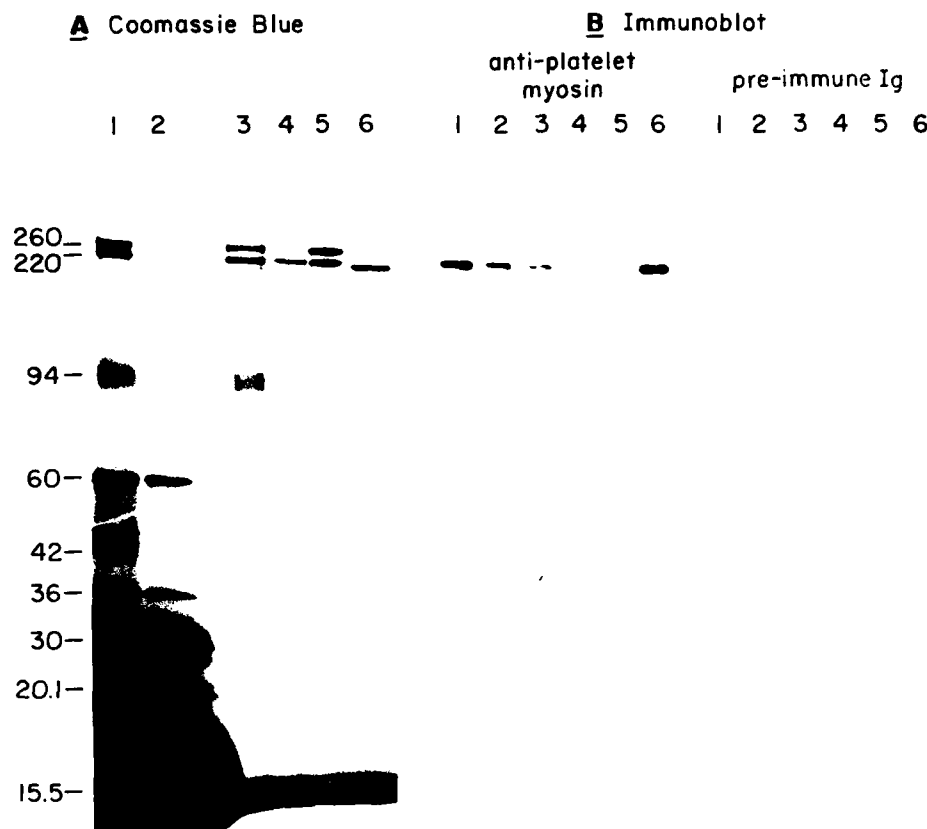


FIGURE 1 Identification of an M_r 200,000 immunoreactive myosin polypeptide in human erythrocytes. (Lane 1) Erythrocytes; (lane 2) cytosol; (lane 3) membranes; (lane 4) erythrocyte ankyrin (1.5 μ g); (lane 5) erythrocyte spectrin (2 μ g); (lane 6) platelet myosin. (Panel A, 1.6 μ g; panel B, 0.08 μ g). Erythrocytes were lysed in 15 vol of lysis buffer and membranes were prepared as described in Materials and Methods. Aliquots of the lysed erythrocytes, the hemolysate (cytosol), and the washed membranes resuspended to the initial lysis volume were added directly to SDS gel electrophoresis sample buffer (14) and heated to 80°C for 5 min. 80- μ l samples of each were electrophoresed on 5–15% acrylamide linear gradient SDS gels in the presence of 4 M urea, and either (A) stained with Coomassie Blue or (B) electrophoretically transferred to nitrocellulose paper as described in Materials and Methods. The nitrocellulose strips were incubated with 2 μ g/ml of affinity-purified antibodies to human platelet myosin, or preimmune Ig, followed by incubation with 125 I-labeled protein A. Immunoreactive bands were detected by autoradiography after exposure of the film for 1 h.

human erythrocytes. Preimmune Ig did not label either the purified platelet myosin (Fig. 1, lane 6) or the cross-reactive polypeptide in the erythrocytes (Fig. 1, lanes 1–3). The immunoreactive polypeptide was not band 2 of spectrin or ankyrin (M_r equivalent to band 2 of spectrin on these gels), since neither purified ankyrin (Fig. 1, lane 4) nor purified spectrin (Fig. 1, lane 5) were labeled by the antimyosin antibodies. These results suggest that the immunoreactive M_r 200,000 polypeptide could be the M_r 200,000 heavy chain of an erythrocyte myosin-homologue.

To determine whether this immunoreactive myosin polypeptide was localized on the membrane or in the cytosol, we lysed erythrocytes and compared immunoblots of whole cells, hemolysates, and membranes (Fig. 1, lanes 1–3). A true cytoplasmic component would be expected to be present in the hemolysate in the same proportion as in the whole cells, whereas a tightly bound membrane component would be expected to be associated exclusively with the washed membranes. Fig. 1 shows that only ~30–40% of the immunoreactive myosin polypeptide was released into the supernatant during hemolysis of erythrocytes in 7.5 mM sodium phosphate, pH 7.5 (Fig. 1, lane 2), while an additional 30–40% was washed off the membranes during the preparation of

ghosts (Fig. 1, lane 3).² This intermediate fractionation behavior might be expected from a component that is loosely bound to the membrane as well as being present in the cytosol. However, a variable proportion of the putative myosin homologue may also be tightly associated with the membranes since ~20–30% of the immunoreactive myosin polypeptide remained associated with the membranes even in well-washed, white ghosts (Fig. 1, lane 3), and inclusion of physiological concentrations of magnesium (2 mM) in the lysis and washing buffers resulted in about a twofold increase in this amount (data not shown).

Immunofluorescence staining of formaldehyde-fixed erythrocytes with the affinity-purified antibodies to myosin demonstrated that the immunoreactive myosin polypeptide was present in all cells (Fig. 2a). The putative erythrocyte myosin-homologue was thus not derived from reticulocytes or from contaminating platelets or neutrophils in the cell preparations. No staining with preimmune Ig was observed under these conditions (Fig. 2c). The antimyosin staining was only observed when the fixed cells were permeabilized with acetone

² Estimated by quantitative immunoblotting procedures as described in Materials and Methods.

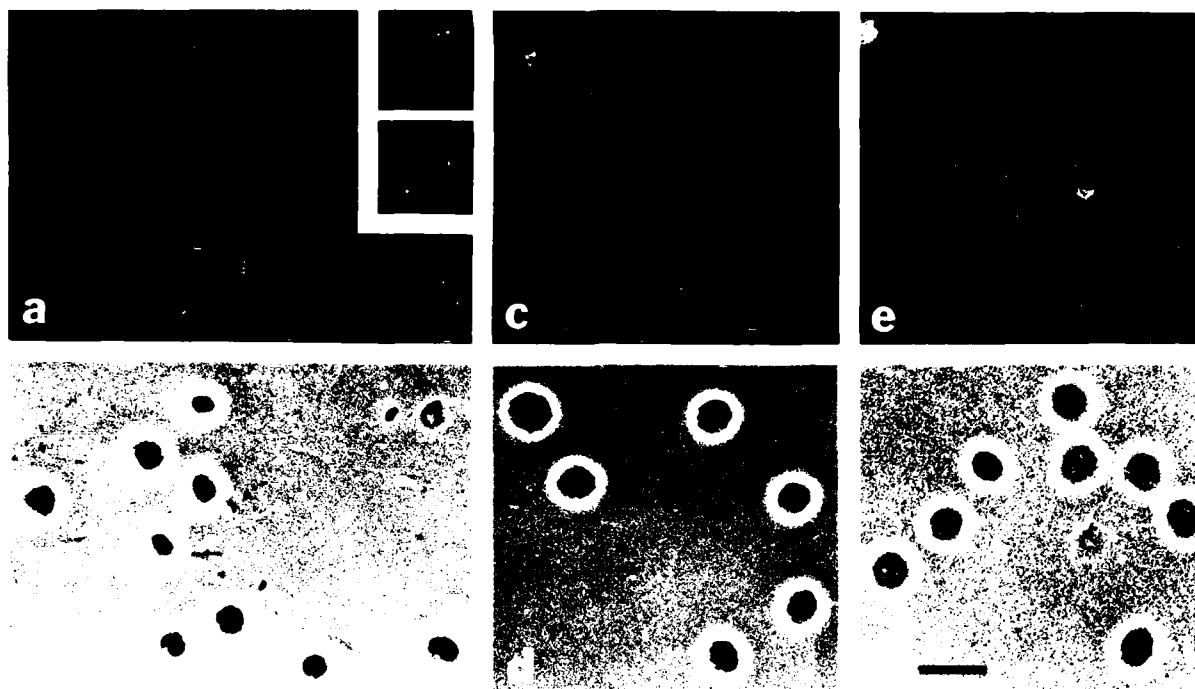


FIGURE 2 Immunofluorescence staining of human erythrocytes with antiplatelet myosin (a), preimmune Ig (c), and antispectrin (e). b, d, and f are phase-contrast micrographs corresponding to a, c, and e. Erythrocytes were fixed with 3% paraformaldehyde followed by acetone at -20°C and incubated with the various rabbit Ig samples at $10\text{ }\mu\text{g/ml}$, followed by rhodamine-conjugated goat anti-rabbit IgG, as described in Materials and Methods. The antispectrin staining in e is actually 50–100-fold brighter than the antimyosin staining in a (estimated by the exposure times used to photograph the cells and to print the negatives), but the micrographs are printed so as to be on the same scale for comparison. (a–f) Bar, $10\text{ }\mu\text{m}$. $\times 9,000$. (Inset) $\times 18,000$.

before incubation with the antibody, indicating that the immunoreactive myosin polypeptide was in the interior of the cell and not adsorbed adventitiously to the cell surface. The antimyosin staining was variable in intensity and was distributed in a granular or punctate pattern in each cell (Fig. 2a, see inset). The small size of the cells and the relatively dim staining made it difficult to determine whether the punctate antimyosin staining was localized in the cytosol and/or associated with the membrane in the fixed cells. The punctate staining pattern was probably not artifactually induced by the fixation/permeabilization protocol because staining with affinity-purified antibodies to spectrin produced a uniform rim-staining pattern (Fig. 2e), which is consistent with the established location of spectrin on the cytoplasmic surface of the membrane (5, 23, 39).

Purification and Partial Characterization of Erythrocyte Myosin

To evaluate the possibility that the immunoreactive myosin polypeptide is the M_r 200,000 heavy chain of an erythrocyte myosin-homologue, we purified the polypeptide from the hemolysate and compared its physical and functional properties with those established for authentic vertebrate myosins (19, 21, 29). The immunoreactive myosin polypeptide was separated from the enormous amount of hemoglobin, as well as numerous other cytosolic proteins in the hemolysate, by DEAE-cellulose chromatography in the presence of 20 mM sodium pyrophosphate, pH 7.5 (Fig. 3A, compare lanes 1 and 2). This procedure also served to concentrate the M_r 200,000 immunoreactive myosin polypeptide by about 25-fold with respect to its original concentration in the hemolysate (<1

$\mu\text{g/ml}$).² The M_r 200,000 polypeptide was then concentrated an additional 10-fold by precipitation with ammonium sulfate at 60% saturation (Fig. 3A, lane 3) and separated from most of the low molecular weight polypeptides by gel filtration in 0.5 M KCl on Sephacryl S-400 (Fig. 3A, lane 4). When more protein was loaded on the gels, two low molecular weight polypeptides (M_r 25,000 and 19,500) were seen to be associated with the purified M_r 200,000 polypeptide (Fig. 3B, lane 1). These polypeptides were present in a molar ratio of 1.09 M_r 25,000:0.90 M_r 19,500:1.0 M_r 200,000 polypeptide,³ and thus presumably represent the two light chains that would be expected to be associated with the M_r 200,000 heavy chain of an erythrocyte myosin molecule. Together, these three polypeptides accounted for $\sim 85\%$ of the Coomassie Blue-staining material in the purified preparation. In the representative experiment shown in Fig. 3, $\sim 0.7\text{ mg}$ of protein was obtained from two units of blood, which represents a recovery of $\sim 18\%$ of the protein present as the M_r 200,000 immunoreactive myosin polypeptide in the hemolysate.²

Structurally, the purified erythrocyte myosin is a typical vertebrate myosin, with two heads and a long rod-like tail $\sim 150\text{ nm}$ long (21, 29, 36), as visualized by low angle rotary shadowing of individual molecules (Fig. 4, left column). The double-headed appearance of the individual molecules, together with the roughly equimolar stoichiometry of the M_r 200,000, 25,000, and 19,500 polypeptides (1:1.09:0.90, see above), suggests that the native molecules are dimers of two heavy chains, each with two associated light chains, as are other myosins. In addition, peptide maps of the M_r 200,000

³ Determined by quantitative elution of dye from the Coomassie Blue-stained protein bands as described by Fenner et al. (12).

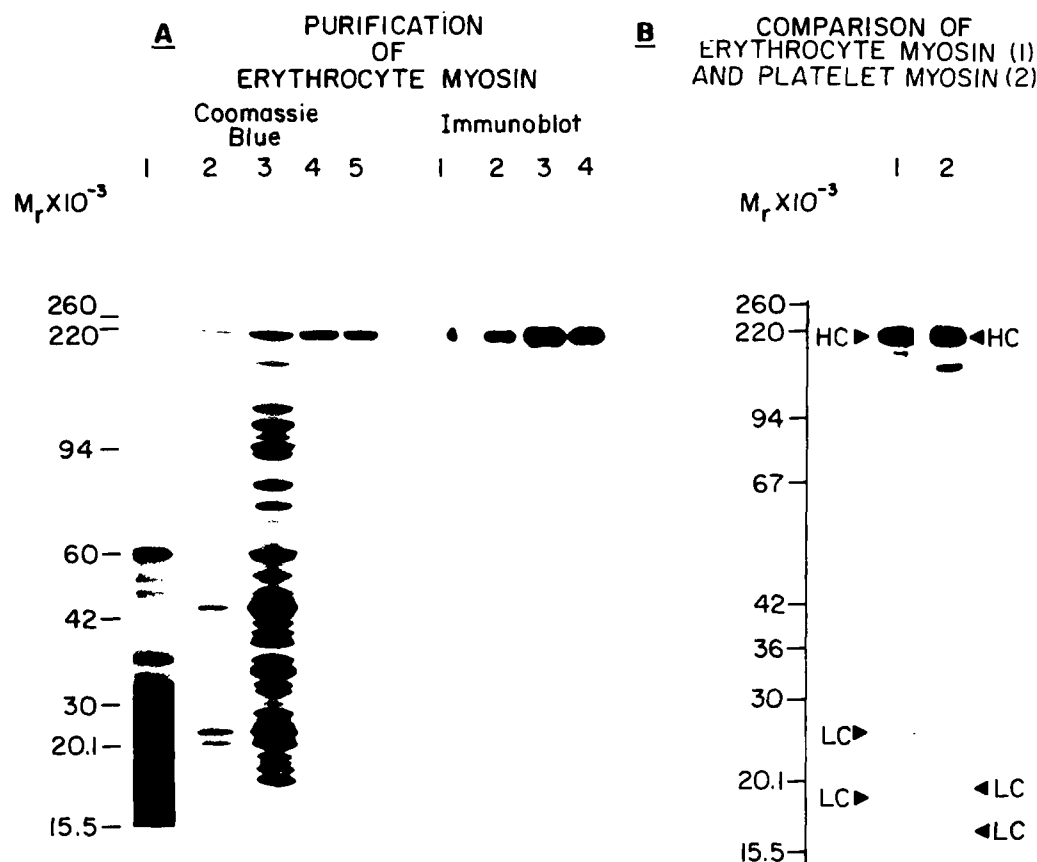


FIGURE 3 (A) Purification of human erythrocyte myosin. Erythrocytes were isolated from two units of whole blood as described by Bennett (6) and lysed in 12 vol of ice-cold 7.5 mM sodium phosphate, 1 mM EDTA, 2 mM DTT, 20 μ g/ml phenylmethylsulfonyl fluoride (pH 7.5), and the membranes were removed by centrifugation for 45 min at 17,000 g (2°C). The hemolysate (3,300 ml) was adsorbed batchwise to DEAE-cellulose equilibrated with 20 mM sodium pyrophosphate, 1 mM EDTA, 2 mM DTT (pH 7.5) for 1 h at 4°C with stirring, and unadsorbed protein (mainly hemoglobin) was removed by several cycles of settling and decanting of the DEAE in this buffer. The DEAE was poured into a column (2.5 \times 18 cm), washed with 5 column volumes of 50 mM NaCl, 20 mM sodium pyrophosphate, 1 mM EDTA, 2 mM DTT (pH 7.5), and then eluted with 7 column volumes of a 50–250 mM NaCl linear gradient in the same buffer, collecting 10-ml fractions. Fractions containing the immunoreactive myosin polypeptide (assayed by immunoblotting procedures) were pooled (150 ml), and the protein was precipitated by addition of 1.5 vol of ice-cold, saturated ammonium sulfate and then collected by centrifugation for 20 min at 17,000 g. The precipitate was resuspended to a 13-ml final vol in 0.5 M KCl, 10 mM Tris, 1 mM EDTA, 1 mM DTT (pH 7.5), and centrifuged for 30 min at 100,000 g. The supernatant was applied to a Sephacryl S-400 column (2.5 \times 85 cm) equilibrated with the same buffer and run at 20 ml/h, collecting 5-ml fractions. Fractions containing the *M_r* 200,000 polypeptide eluted at \sim 1.5 *V₀* and were pooled (40 ml) and concentrated 5–10-fold to 0.1–0.2 mg/ml by dialysis against solid sucrose. The purified protein was stored on ice after dialysis against 0.5 M KCl, 10 mM 3-(*N*-morpholino) propane sulfonic acid, 1 mM EDTA, 1 mM DTT (pH 7.0) and was stable for at least 3 wk. Samples of hemolysate (80 μ l) [lane 1], the DEAE pool (40 μ l) [lane 2], the ammonium sulfate-concentrated material (20 μ l) [lane 3], and the purified *M_r* 200,000 polypeptide (2 μ g) [lane 4] were electrophoresed on 5–15% acrylamide linear gradient SDS gels containing 4 M urea and either stained with Coomassie Blue (left) or transferred to nitrocellulose and labeled with 4 μ g/ml platelet myosin and ¹²⁵I-labeled protein A (right) as described in Materials and Methods. One tenth as much protein was loaded for the immunoblots, and the immunoreactive bands were detected after exposure of the autoradiograms for only 30 min. Lane 5 is 2 μ g of purified human platelet myosin for comparison. (B) Comparison of 6 μ g each of purified human erythrocyte myosin (lane 1) and human platelet myosin (lane 2) on 7.5–15% acrylamide linear gradient SDS gels in the absence of urea (14). HC, heavy chains; LC, light chains.

heavy chain of the purified erythrocyte myosin and of platelet myosin were found to be nearly identical (Fig. 5), indicating a high degree of structural homology between the two proteins. However, these proteins are distinct in that the molecular weights determined for the platelet myosin light chains on 7.5–15% acrylamide linear gradient SDS gels (*M_r* 20,000 and 17,000; Fig. 3B, lane 2) were different from those determined for the erythrocyte myosin light chains (*M_r* 25,000 and 19,500; Fig. 3B, lane 1).

Dialysis of the purified erythrocyte myosin into low salt led

to formation of typical bipolar myosin filaments (0.3–0.4 μ m long) with the heads at each end and a central bare zone in the middle (Fig. 4, middle and right column). Occasionally, possible intermediate stages in the formation of these filaments were observed in the rotary-shadowed specimens. For example, two molecules are associated via their tails in the bottom left panel of Fig. 4, and the head end of an individual myosin molecule is splayed out from the bipolar filament while the tail region remains attached in the filaments depicted in the bottom two panels of the middle column in Fig.

4. The looser association of the molecules in the rotary-shadowed specimens as compared with the negatively stained specimens may be due to the somewhat different dialysis conditions used for the sample preparations (0.1 M ammonium formate, pH 7.5, versus 50 mM KCl, 2 mM MgCl₂, pH 7.0), or it may be an artifact of the respective electron microscopic techniques.

The purified erythrocyte myosin exhibited a characteristic pattern of myosin ATPase activities, with a Ca²⁺-activated, Mg²⁺-inhibited ATPase activity at both high and low salt, and activation by high concentrations of KCl but not NaCl in the absence of divalent cations (2 mM EDTA) (Table I). The Ca²⁺-ATPase activity in 0.5 M KCl of the erythrocyte myosin was higher than the EDTA-ATPase activity measured in 0.5 M KCl (0.48 and 0.38 $\mu\text{mol}/\text{min}$ per mg, respectively). This is the reverse of the relative Ca²⁺ and EDTA-ATPase activities of platelet myosin measured under similar condi-

tions (0.35 and 0.50 $\mu\text{mol}/\text{min}$ per mg, respectively, see reference 28). The addition of rabbit skeletal muscle F-actin (1 mg/ml) to purified erythrocyte myosin had no effect on the low Mg²⁺-ATPase activity of erythrocyte myosin that was measured in 60 mM KCl, 2 mM MgCl₂, pH 7.0 (<0.01 $\mu\text{mol}/\text{min}$ per mg).

Determination of the Number of Copies of Myosin per Cell

The purified erythrocyte myosin was used as a standard in a quantitative immunoblotting assay to determine the amount of myosin in erythrocytes (Materials and Methods). As shown in Table II, the amount of the *M*_r 200,000 heavy chain of erythrocyte myosin detected was directly proportional to the microliters of cell equivalents electrophoresed and transferred to nitrocellulose, which demonstrates that the assay is operating in both antimyosin antibody and ¹²⁵I-protein A excess. Additionally, this also shows that the co-migrating spectrin (band 2) and ankyrin polypeptides are not interfering with the transfer or antibody labeling of the erythrocyte myosin heavy chain. The molar ratio of the *M*_r 200,000 polypeptide to spectrin was calculated with respect to the micrograms of band 1 of spectrin in each sample because there are no polypeptides co-migrating with band 1 of spectrin on these SDS gels of erythrocytes. The average value for the ratio of spectrin to myosin calculated from the values in Table I was 32.1 spectrin dimers/myosin molecule (dimer of two heavy chains). Since there are 200,000 molecules of spectrin dimer per cell (5), the number of molecules of myosin per cell would be 6,240. This is a ratio of about 80 actin monomers for every myosin molecule, assuming there are 500,000 copies of actin per cell (5, 26).

DISCUSSION

The possibility that erythrocytes contain myosin has been discussed since 1960 when Nakao et al. (22) first observed the reversible ATP-dependent discocyte-echinocyte shape transformations of human erythrocytes. The ability of isolated membranes (ghosts) to undergo similar ATP-dependent shape transformations (24, 34, 37), as well as ATP-dependent endocytosis (25, 31), led numerous investigators to hypothesize

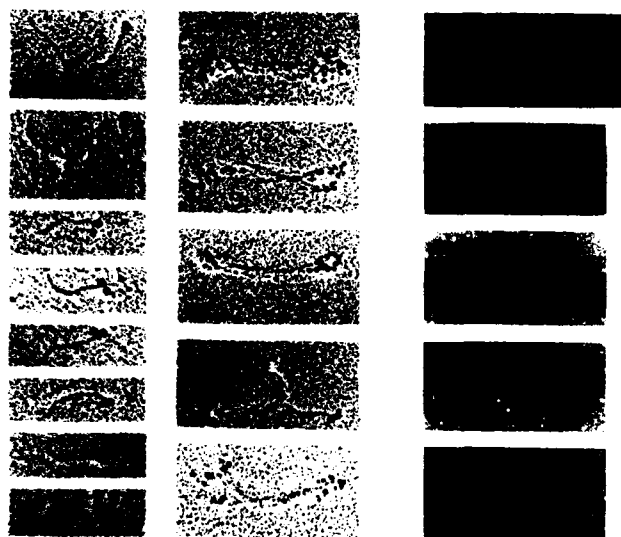


FIGURE 4 Electron micrographs of low angle, rotary-shadowed individual human erythrocyte myosin molecules (left) and myosin filaments (middle), and of negatively stained myosin filaments (right). Bar, 200 nm. $\times 100,000$.

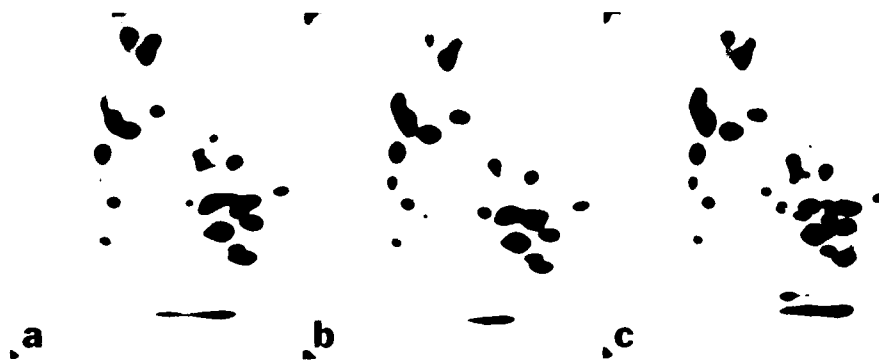


FIGURE 5 Two-dimensional peptide maps of ¹²⁵I-labeled chymotryptic peptides of human erythrocyte myosin heavy chain (a), human platelet myosin heavy chain (b), and a mixture of peptides from platelet and erythrocyte myosin heavy chains (c). Myosin from platelets and erythrocytes (50 pmol each) was denatured in 0.1% (wt/vol) SDS, radiolabeled with 1 mCi of ¹²⁵I by using chloramine-T as an oxidant, and electrophoresed on an SDS polyacrylamide gel. The ¹²⁵I-labeled heavy chains were localized by staining with Coomassie Blue, cut from the gel, and digested with 50 $\mu\text{g}/\mu\text{l}$ alpha-chymotrypsin in 50 mM ammonium formate, 1 mM NaH₂PO₄ for 18 h at 37°C. The digest was lyophilized and analyzed by electrophoresis (horizontal dimension) and chromatography (vertical dimension) as described (11).

that cell shape and membrane properties were influenced by a membrane-associated actomyosin contractile apparatus. At one point, it was suggested that spectrin might be a myosin-like protein (15) and that the actin-spectrin network underlying the membrane could be the erythrocyte membrane analogue to actomyosin contractile systems in other cells (33, 34). However, the extensive work on the physical and functional properties of spectrin (18) and the recent identification of spectrin-like proteins in nonerythrocyte cells and tissues (4, 5) have made it abundantly clear that spectrin is not myosin. In this report we have established the presence in the human erythrocyte of an authentic vertebrate myosin, based on cross-reaction with affinity-purified antibodies to human platelet myosin and characterization of the structural and functional properties of the purified protein. Myosin is an endogenous component of mature human erythrocytes, based on immunofluorescence localization of myosin in all cells, and is present with respect to the actin on the erythrocyte membrane in an amount comparable to actin/myosin ratios in other nonmuscle cells (molar ratio = 80/1; see reference 29). Our work confirms and extends a preliminary report by Kirkpatrick and Sweeney (17) that erythrocyte cytosol contained myosin, and also presumably accounts for previous observations of myosin-like ATPase activities in crude preparations of spectrin from erythrocyte membranes (3, 30).

In retrospect, there are several reasons why the presence of myosin in the erythrocyte has been previously overlooked. First, the intensity of antimyosin staining of erythrocytes is considerably less intense than that of platelets or neutrophils in samples of whole blood processed for indirect immunofluorescence (V. Fowler, unpublished data). Second, the presence of interfering ATPase activities, and the similarity in molecular weight on SDS gels of the myosin heavy chain to the major cytoskeletal proteins, spectrin and ankyrin, makes it impossible to employ the usual criteria for initial identification of myosin. Finally, attention has focused on structural proteins that are tightly associated with the membrane, while the majority of the erythrocyte myosin is released into the supernatant during hemolysis and preparation of membranes under hypotonic conditions (7.5 mM sodium phosphate, pH 7.5).

In common with myosins isolated from various nonmuscle cells, the Mg^{++} -ATPase activity of erythrocyte myosin is not enhanced by the addition of rabbit skeletal muscle F-actin (19, 29). Actin activation of the Mg^{++} -ATPase activity of platelet and other cytoplasmic myosins, as well as smooth muscle myosin, occurs only after the M_r 20,000 light chain of the myosin has been phosphorylated by a calcium- and calmodulin-dependent protein kinase (1). Thus, it is possible that the M_r 19,500 light chain of erythrocyte myosin could be

TABLE I
ATPase Activity of Erythrocyte Myosin

	2 mM EDTA	10 mM CaCl ₂	10 mM MgCl ₂
0.5 M KCl	0.376	0.478	<0.01
0.06 M KCl	0	0.406	<0.01
0.5 M NaCl	0.118	0.204	0

ATPase activities (μ mol/min per mg) were determined by using 25 μ g/ml of purified erythrocyte myosin in a buffer containing 10 mM 3-(N-morpholino)propane sulfonic acid, 1 mM ATP, pH 7.0, ions as specified above, and 0.5 μ Ci/ml [γ -³²P]ATP. The radioactivity released as P_i was determined after incubation for 15 and 30 min as described by Agre et al. (2), and was corrected for nonenzymatic P_i release in the absence of myosin.

TABLE II
Quantitation of the Amount of Myosin in the Erythrocyte

	Cell equivalents (μ l)*		
	1.0	1.5	2.0
Spectrin band 1 (μ g) [†]	0.66	0.99	1.32
Erythrocyte myosin (μ g) [‡] heavy chain	0.030	0.048	0.066
Spectrin dimer/myosin (mol/mol) [§]	33.8	31.7	30.8
Molecules myosin per cell [¶]	5,917	6,309	6,494

* Calculated from the microliters of sample electrophoresed for each determination and the volume of packed cells used to prepare the initial gel sample.

[†] Determined by the dye elution method of Fenner et al. (12) from a standard curve constructed by electrophoresing known quantities of purified spectrin in parallel with the gel samples of the erythrocytes.

[‡] Determined by a quantitative immunoblotting procedure as described in Materials and Methods.

[§] Calculated assuming M_r 260,000 for band 1 of spectrin and M_r 200,000 for the heavy chain of erythrocyte myosin, and that each spectrin molecule (dimer) contains one band 1 polypeptide whereas each myosin molecule contains two M_r 200,000 heavy chains.

[¶] Calculated assuming 200,000 spectrin dimers per cell (5).

homologous to the M_r 20,000 regulatory light chains of other cytoplasmic myosins, and as isolated, be in the dephosphorylated state. Regulation of the level of phosphorylation of the M_r 19,500 light chain of erythrocyte myosin by a calcium- and calmodulin-dependent protein kinase, coupled with a myosin light chain phosphatase, could provide a mechanism for calcium control of erythrocyte actomyosin ATPase activity, as has been described for platelet and smooth muscle actomyosin systems (1). However, the presence in erythrocyte myosin of a light chain of apparent M_r 25,000 on SDS gels, similar to vertebrate skeletal and cardiac muscle myosins (21, 38), and unlike other previously characterized cytoplasmic or smooth muscle myosins (19, 29), suggests that other regulatory mechanisms should be considered. For example, it is possible that actin activation of the Mg^{++} -ATPase activity of erythrocyte myosin could be specific for erythrocyte membrane actin, which consists exclusively of the beta-isoelectric variant (reference 27 and V. Fowler, unpublished data), as suggested by Schrier et al. (32). Calcium regulation of erythrocyte actomyosin ATPase activity could then be provided by an actin-linked erythrocyte troponin-tropomyosin system, as discussed previously (14). Clearly, these regulatory mechanisms are not mutually exclusive, and additional myosin or actin-linked mechanisms for control of erythrocyte actomyosin ATPase activity might also exist (19, 29).

Myosin in the human erythrocyte could function, together with the membrane-associated actin protofilaments, in an actomyosin contractile apparatus responsible for ATP-dependent discocyte-echinocyte changes in cell shape and membrane properties (25, 31, 34, 37). Additionally, the passage of erythrocytes through the narrow sinusoids in the spleen may not be entirely a passive process driven by hydrostatic pressure, but may be facilitated by energy-dependent actomyosin contractions that are triggered by increases in intracellular calcium resulting from enhanced passive calcium permeability induced by physiological shear stresses (20). Such a hypothesized actomyosin contractile apparatus is probably not permanently assembled on the erythrocyte membrane, since much of the myosin is released into the supernatant after hemolysis of fresh, ATP-replete biconcave cells. The interac-

tion of myosin with the erythrocyte membrane cytoskeleton is likely to be complex and regulated at several levels: the ATP-dependent interaction of myosin heads with the actin protofilaments in the membrane skeleton (actomyosin ATPase); the self-association of molecules into bipolar filaments; and the association of filaments or individual myosin molecules via their tails to a nonactin site on the membrane. It is tempting to speculate that the increases in intracellular calcium and depletion of ATP levels that are correlated with discocyte-echinocyte shape transformations of erythrocytes (22, 24, 37) could be functionally related to assembly and activity of an actomyosin contractile apparatus on the erythrocyte membrane.

Although there is no precedent for the organization and functioning of a membrane-associated contractile apparatus, the ability of erythrocyte myosin to form bipolar filaments at the concentrations of myosin estimated to be present in the erythrocyte ($\sim 50 \mu\text{g/ml}$)⁴ raises the possibility that force production and membrane movements could result from ATP-dependent sliding of bipolar myosin filaments past antiparallel actin filaments in the membrane skeleton. The punctate character of the antimyosin staining of erythrocytes and the ratio of actin to myosin (80 monomers/myosin molecule; or 1,200 monomers/1 myosin filament of 15 monomers; reference 29) suggest that actomyosin interactions might occur at specialized sites in the membrane skeleton. Localized contractions could be transmitted through the cytoskeletal network via the multiple spectrin-band 4.1 linkages between the actin protofilaments, and tension could be exerted on the membrane via the specific association of spectrin with ankyrin. Alternatively, individual myosin molecules could be attached directly to a membrane site via their tails, leaving their heads free to interact with the actin protofilaments. The relationship of such hypothesized calcium-activated actomyosin contractions of the membrane cytoskeletal network to the previously observed inhibition of spectrin-band 4.1-actin gelation by micromolar calcium (13) is not immediately apparent. It is possible that the intracellular free calcium ion concentration could regulate spectrin-band 4.1-actin interactions concurrently with actomyosin contractions in a membrane-associated counterpart of the solation-contraction coupling mechanism that has been proposed to explain amoeboid movements (8, 9, 16). Clearly, evaluation of these ideas will require extensive biochemical and ultrastructural investigation of the interaction of myosin with the membrane and with the actin filaments in the membrane skeleton. In particular, the relationship of actomyosin interactions to the spectrin-band 4.1-actin linkages in the membrane cytoskeleton, as well as the locations and associations of potential regulatory proteins such as tropomyosin (14) or troponins, will need to be defined.

We acknowledge Thomas D. Pollard and Doug Murphy for their gift of antibodies to human platelet myosin for a preliminary immunoblot of erythrocyte membranes, and Rebecca Wagner for technical assistance in performing the initial immunoblots. We also thank Brian E. Burke for his advice in working out the immunofluorescence procedures, Peter C. Agre for the affinity-purified antibodies to spectrin, Tom Urquhart for the photography, and Arlene Daniel for the typing.

⁴ Calculated from the number of copies of myosin per cell (6,000, see Results) and a cell volume of $85 \mu\text{m}^3$.

This work was supported by grants from the National Institutes of Health to V. M. Fowler (R01 GM31364) and to V. Bennett (R01 AM29808 and Research Career Development Award K04 AM00926), and by a grant from the Army to V. Bennett (DAMD17-83-C-3209).

Received for publication 23 July 1984, and in revised form 30 August 1984.

Note added in Proof: In a recent experiment by Albert J. Wong, Daniel P. Kiehart, and Thomas D. Pollard (*J. Biol. Chem.*, in press), phosphorylation of the M_r 19,500 light chain was observed to be correlated with the actin-activated ATPase activity of erythrocyte myosin.

REFERENCES

- Adelman, R. S., and E. Eisenberg. 1980. Regulation and kinetics of the actin-myosin-ATP interaction. *Annu. Rev. Biochem.* 49:921-956.
- Agre, P., K. Gardner, and V. Bennett. 1983. Association between human erythrocyte calmodulin and the cytoplasmic surface of human erythrocyte membranes. *J. Biol. Chem.* 258:6258-6265.
- Avissar, N., A. deVries, Y. Ben-Shaul, and I. Cohen. 1975. Actin-activated ATPase from human erythrocytes. *Biochim. Biophys. Acta* 375:35-43.
- Baines, A. J. 1983. The spread of spectrin. *Nature (Lond.)* 301:377-378.
- Bennett, V. 1983. The human erythrocyte as a model system for understanding membrane-cytoskeleton interactions. In *Cell Membranes: Methods and Reviews*, E. Elson, W. Frazier, and L. Glaser, editors. Plenum Press, New York.
- Bennett, V. 1983. Proteins involved in membrane-cytoskeleton association in human erythrocytes: spectrin, ankyrin, and band 3. *Methods Enzymol.* 96:313-324.
- Cohen, C. M. 1983. The molecular organization of the red cell membrane skeleton. *Semin. Hematol.* 20:141-158.
- Condeelis, J. S. 1981. Reciprocal interactions between the actin lattice and cell membrane. *Neurosci. Res. Prog. Bull.* 19(1):83-99.
- Condeelis, J. S., and D. L. Taylor. 1977. The contractile basis of amoeboid movement. V. The control of gelation, solation, and contraction in extracts from *Dictyostelium discoideum*. *J. Cell Biol.* 74:901-927.
- Davis, J. Q., and V. Bennett. 1984. Brain ankyrin. Purification of a 72,000 M_r spectrin-binding domain. *J. Biol. Chem.* 259:1874-1881.
- Elder, J. H., R. A. Pickett II, J. Hampton, and R. A. Lerner. 1977. Radioiodination of proteins in single polyacrylamide gel slices. Tryptic peptide analysis of all the major members of complex multicomponent systems using microgram quantities of total protein. *J. Biol. Chem.* 252:6510-6515.
- Fenner, C., R. R. Traut, D. T. Mason, and J. Wikman-Coffelt. 1975. Quantification of Coomassie blue stained proteins in polyacrylamide gels based on analysis of eluted dye. *Anal. Biochem.* 63:595-602.
- Fowler, V., and D. L. Taylor. 1980. Spectrin plus band 4.1 cross-link actin. Regulation by micromolar calcium. *J. Cell Biol.* 85:361-376.
- Fowler, V. M., and V. Bennett. 1984. Erythrocyte membrane tropomyosin. Purification and properties. *J. Biol. Chem.* 259:5978-5989.
- Guidotti, G. 1972. Membrane proteins. *Annu. Rev. Biochem.* 41:731-752.
- Hellewell, S. B., and D. L. Taylor. 1979. The contractile basis of amoeboid movement. VI. The solation-contraction coupling hypothesis. *J. Cell Biol.* 83:633-648.
- Kirkpatrick, F. H., and M. L. Sweeney. 1980. Cytoplasmic and membrane-bound erythrocyte myosin(s). *Fed. Proc.* 39:2049a. (Abstr.)
- Knowles, W. S., L. Marchesi, and V. T. Marchesi. 1983. Spectrin: structure, function, and abnormalities. *Semin. Hematol.* 20:159-174.
- Korn, E. D. 1978. Biochemistry of actomyosin-dependent cell motility. *Proc. Natl. Acad. Sci. USA* 75:588-599.
- Larsen, F., L. S. Katz, B. D. Roufogalis, and D. E. Brooks. 1981. Physiological shear stresses enhance the Ca^{2+} permeability of human erythrocytes. *Nature (Lond.)* 294:667-668.
- Lowey, S. 1971. Myosin: Molecule and Filament. In *Subunits in Biological Systems*, S. N. Timasheff and G. D. Fasman, editors. Marcel Dekker, Inc., New York. Part A:201-259.
- Nakao, M., T. Nakao, S. Yamazoe, and H. Yoshikawa. 1961. Adenosine triphosphate and the shape of erythrocytes. *J. Biochem. (Tokyo)* 49:487-492.
- Nicolson, G. L., V. T. Marchesi, and S. J. Singer. 1971. The localization of spectrin on the inner surface of human red blood cell membranes by ferritin-conjugated antibodies. *J. Cell Biol.* 51:265-272.
- Palek, J., W. A. Curby, and F. J. Lionetti. 1971. Effects of calcium and adenosine triphosphate on volume of human red cell ghosts. *Am. J. Physiol.* 220:19-26.
- Penniston, J. T., and D. E. Green. 1968. The conformational basis of energy transformations in membrane systems. IV. Energized states and pinocytosis in erythrocyte ghosts. *Arch. Biochem. Biophys.* 128:339-350.
- Pinder, J. C., and W. B. Gratzer. 1983. Structural and dynamic states of actin in the erythrocyte. *J. Cell Biol.* 96:768-775.
- Pinder, J. C., E. Ungewickell, and W. B. Gratzer. 1978. The spectrin-actin complex and erythrocyte shape. *J. Supramol. Struct.* 8:439-445.
- Pollard, T. D., S. M. Thomas, and R. Niederman. 1974. Human platelet myosin. I. Purification by a rapid method applicable to other non-muscle cells. *Anal. Biochem.* 60:258-266.
- Pollard, T. D., and R. R. Weising. 1974. Actin and myosin in non-muscle cells. *CRC Crit. Rev. Biochem.* 2:1-65.
- Rosenthal, A. S., F. M. Kregenow, and H. L. Moses. 1970. Some characteristics of a Ca^{2+} -dependent ATPase activity associated with a group of erythrocyte membrane proteins which form fibrils. *Biochim. Biophys. Acta* 196:254-262.
- Schnier, S. L., K. G. Bensch, M. Johnson, and I. Junga. 1975. Energized endocytosis in human erythrocyte ghosts. *J. Clin. Invest.* 56:8-22.
- Schnier, S. L., B. Hardy, I. Junga, and L. Ma. 1981. Actin-activated ATPase in human

red cell membranes. *Blood* 58:953-962.

33. Sheetz, M. P., R. G. Painter, and S. J. Singer. 1976. Relationships of the spectrin complex of human erythrocyte membranes to the actomyosins of muscle cells. *Biochemistry* 15:4486-4492.
34. Sheetz, M. P., and S. J. Singer. 1977. On the mechanisms of ATP-induced shape changes in human erythrocyte membranes. I. Role of spectrin complex. *J. Cell Biol.* 73:638-646.
35. Shen, B. W., R. Josephs, and T. I. Steck. 1984. Ultrastructure of unit fragments of the skeleton of the human erythrocyte membrane. *J. Cell Biol.* 99:810-821.
36. Shotton, D. M., B. E. Burke, and D. Branton. 1979. The molecular structure of human erythrocyte spectrin. Biophysical and electron microscopic studies. *J. Mol. Biol.* 131:303-329.
37. Weed, R. I., P. I. LaCelle, and E. W. Merrill. 1969. Metabolic dependence of red cell deformability. *J. Clin. Invest.* 48:795-809.
38. Weeds, A. 1980. Myosin light chains, polymorphism and fibre types in skeletal muscles. In *Plasticity of Muscle*, D. Pette, editor. Walter de Gruyter & Co., New York: 55-68.
39. Ziparo, E., A. Lemay, and V. T. Marchesi. 1978. The distribution of spectrin along the membranes of normal and echinocytic human erythrocytes. *J. Cell Sci.* 34:91-101.

***Plasmodium falciparum* Malaria: Band 3 as a Possible Receptor During Invasion of Human Erythrocytes**

Vincent C. N. Okoye* and Vann Bennett

***Plasmodium falciparum* Malaria: Band 3 as a Possible Receptor During Invasion of Human Erythrocytes**

Abstract. Human erythrocyte band 3, a major membrane-spanning protein, was purified and incorporated into liposomes. These liposomes, at nanomolar concentrations of protein, inhibited invasion of human erythrocytes *in vitro* by the malaria parasite *Plasmodium falciparum*. Liposomes containing human band 3 were ten times more effective in inhibiting invasion than those with pig band 3 and six times more effective than liposomes containing human erythrocyte glycophorin. Liposomes alone or liposomes containing erythrocyte glycolipids did not inhibit invasion. These results suggest that band 3 participates in the invasion process in a step involving a specific, high-affinity interaction between band 3 and some component of the parasite.

Malaria remains a major public health problem in many areas of the world, with an estimated 150 million cases resulting in 2 million deaths each year (1). Victims are inoculated by mosquito bite with the sporozoite stage of the malarial parasite, and the sporozoites rapidly invade hepatic parenchymal cells and differentiate into merozoites. The merozoites are released into the circulation, where they invade erythrocytes. Infected erythrocytes soon rupture, releasing multiple merozoites that invade other erythrocytes, leading to chronic parasitemia. Invasion of erythrocytes is a multistep process that involves (i) attachment of merozoites to the erythrocyte membrane in a random orientation; (ii) reorientation of the attached merozoites such that the apical end of the parasite is opposed to the erythrocyte membrane; (iii) formation of a junction between the apical end of the merozoite and the erythrocyte membrane; and (iv) invagination of the erythrocyte membrane around the attached merozoite to form a vacuole inside the erythrocyte (2).

Several lines of evidence indicate that the invasion process requires specific interactions between the merozoite and the host erythrocyte (3). Erythrocyte membrane proteins glycophorins A, B, and C have been implicated as one of the attachment sites for *Plasmodium falciparum* (3), the species that causes the most virulent form of human malaria. Invasion of erythrocytes by *P. falciparum* *in vitro* has been reduced by genetic

deficiency of glycophorins (4), digestion of glycophorin with trypsin or neuraminidase (3), and addition of isolated glycophorin to the assay medium (5). Friedman *et al.* (6) suggested that glycophorins A and B are involved in a relatively nonselective, charge-mediated attachment between merozoites and the red cell membrane, since various polyanions also inhibit invasion and since orosomucoid, a serum sialoglycoprotein unrelated to glycophorin, restores the invasion capacity of erythrocytes depleted of glycophorins (6).

Band 3, a major cell-surface protein in erythrocyte membrane, is a logical candidate to mediate specific red cell associations with malarial parasites. In support of this idea, Miller *et al.* (7) found that monoclonal antibody against rhesus monkey band 3 blocks invasion of rhesus erythrocytes by *Plasmodium knowlesi* parasites. We report here that human erythrocyte band 3 incorporated into liposomes is a potent inhibitor of invasion of human erythrocytes by *P. falciparum*, further supporting the hypothesis that band 3 participates in a high-affinity interaction with merozoite surface components.

Band 3 was purified from human erythrocyte ghosts by selective extraction of peripheral membrane proteins, followed by solubilization of membranes with nonionic detergent and fractionation of the detergent extract by ion-exchange chromatography (Fig. 1). Band 3 is not soluble in the absence of deter-

gent and therefore cannot be added directly to invasion assays. However, it is possible to incorporate band 3 into artificial phospholipid bilayer vesicles (liposomes), which maintain the protein in a native state in the absence of detergent.

Fig. 1. Purification of human erythrocyte band 3 and incorporation of band 3 into liposomes. Potassium iodide-extracted inside-out membrane vesicles prepared from 40 ml of human erythrocyte ghosts (8) were solubilized at 4°C in 50 ml of 0.5 percent (by volume) Triton X-100, 10 mM sodium phosphate, 1 mM sodium EDTA, 1 mM dithiothreitol, and 1 mM NaN_3 (pH 7.5). The 100,000g supernatant of this extract was applied to a 15-ml column of DEAE-cellulose equilibrated in solubilization buffer. The column was washed with two bed volumes of buffer and eluted with a linear gradient of NaCl (0.1 to 0.3M) dissolved in solubilization buffer. Fractions were monitored for protein and analyzed by SDS electrophoresis (8). Fractions containing glycophorin (fractions 4 and 5) or band 3 (fractions 11 to 15) were pooled and the proteins were incorporated into liposomes by removal of Triton X-100 on Bio beads followed by addition of egg lecithin and sodium cholate and extensive dialysis (9). The liposomes were resuspended in phosphate-buffered saline. Samples were analyzed by SDS-polyacrylamide gel electrophoresis and the gels were stained with Coomassie blue or PAS to visualize sialoglycoproteins. Lane 1, erythrocyte ghosts; lane 2, potassium iodide-extracted vesicles; lane 3, Triton X-100 extract; lanes 4 to 16, fractions from DEAE chromatography; and lane 17, liposomes containing band 3.

Band 3 and glycophorin (isolated by the same procedure as for band 3) were incorporated into liposomes by the procedure of Yu and Branton (9), which yields single-walled liposomes 40 to 80 nm in diameter. Band 3 reconstituted by

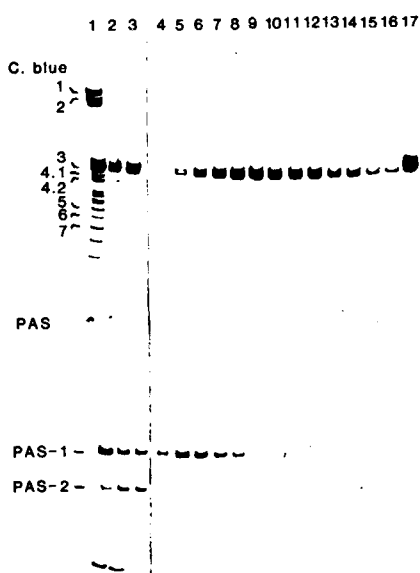
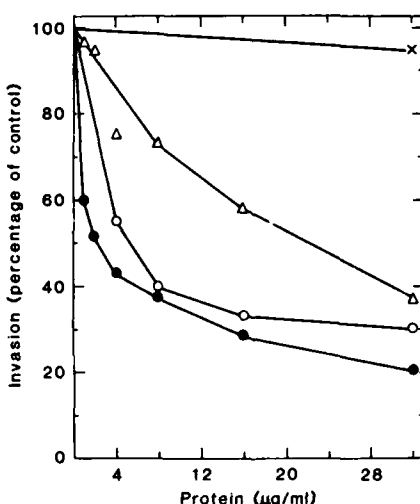


Fig. 2. Effect on reinvasion of erythrocytes by *P. falciparum* malarial parasites of increasing concentrations of liposomes containing human erythrocyte band 3 (●), human erythrocyte glycophorin (○), pig erythrocyte band 3 (△), or no protein (x). The Camp strain of *P. falciparum* was cultured (10) in RPMI 1640 medium supplemented with 10 percent human A⁺ serum (heat-inactivated at 56°C for 30 minutes). Synchronized cultures were obtained by treating asynchronous cultures with sorbitol (11). The schizonts were isolated free of ring forms (immature parasites) by layering the culture mixture over 4 ml of a 15 percent metrizamide gradient and the gradient was centrifuged at 300g and 20°C for 15 minutes. After centrifugation the dark band at the metrizamide-medium interphase (the layer of schizonts) was aspirated in a laminar flow hood, washed once in 10 volumes of RPMI 1640 complete medium, and diluted to a concentration of 2.5×10^7 schizonts per milliliter. Reinvasion by merozoites was assayed in 10-mm microtiter wells. Washed human O⁺ erythrocytes were suspended to a 4 percent hematocrit in RPMI 1640 complete medium containing 10 percent human A⁺ serum. To each well was added 25 μ l of the 4 percent cell suspension, 25 μ l of phosphate-buffered saline, various concentrations of liposomes containing human or pig band 3 protein glycophorin, or liposomes at equivalent dilution but lacking protein. Schizonts (50 μ l; 2.5×10^7 per milliliter) were added to each well, making the final erythrocyte concentration 1 percent and the initial parasitemia between 1.0 and 2 percent. The mixtures were mixed thoroughly and incubated for 3 hours in air with 6 percent O_2 and 5 percent CO_2 . During the 3-hour incubation the contents of the wells were resuspended for 15 seconds every 30 minutes. After 3 hours of incubation most of the medium in each well was carefully removed and smears were made of the cells. The smears were air-dried, flushed with anhydrous methanol, dried again, and stained with Giemsa stain, and the number of intracellular ring stages of the parasites were counted per 10,000 erythrocytes. Data are expressed as the percentage of invasion relative to control wells with buffer added and are means of triplicate determinations. The level of control invasion in this experiment was 774 ring stages per 10,000 erythrocytes.



this method forms intramembrane particles indistinguishable from particles in native membranes (8).

Invasion of human erythrocytes with cultures of *P. falciparum* (Camp strain, Vietnam) (9) synchronized by sorbitol (10) was measured (Fig. 2). Human erythrocyte band 3 inhibited invasion 50 percent at 2 μ g per milliliter of protein, which is about 11 nM band 3 dimer. Invasion was inhibited 80 percent at the highest concentration of band 3 tested. Equivalent inhibition by human band 3 was measured with 12 different preparations of liposomes with band 3 from different donors.

Several controls demonstrated the specificity of the inhibition by human band 3. First, liposomes without protein, prepared under identical conditions and at equivalent dilutions, gave little inhibition. Second, liposomes prepared with pig erythrocyte band 3 were ten times less effective, with 50 percent inhibition at 20 μ g per milliliter of protein (110 nM band 3 dimer). Finally, liposomes containing erythrocyte glycolipid did not inhibit invasion. Thus inhibition required band 3 in addition to lipid, and human band 3 was much more effective than a closely related band 3 from a species resistant to *P. falciparum* malaria. Band 3 in red cells has two domains: an externally oriented domain that is relatively resistant to protease and an internal region facing the cytoplasm that is released by limited proteolysis (11). The external domain of band 3 in liposomes was responsible for inhibition of invasion, since unaltered inhibition was obtained with mildly proteolysed band 3 liposomes that had lost any exposed cytoplasmic domain.

Liposomes containing human glycophorin also blocked invasion, but less actively than those containing human band 3 (Fig. 2). Fifty percent inhibition of invasion by glycophorin required 5 μ g/ml (80 nM), a concentration about seven times higher than that for human band 3. The activity of glycophorin in blocking invasion, although weaker than that of band 3, was comparable to or greater than that reported previously (5).

These experiments confirm the ability of glycophorin to inhibit invasion of erythrocytes by *P. falciparum* and demonstrate that band 3 incorporated into liposomes also blocks invasion at substantially lower concentrations than those of glycophorin. Analysis on sodium dodecyl sulfate (SDS) gels stained with Coomassie blue or periodic acid-Schiff reagent (PAS) showed the band 3 in the liposomes to be 90 percent pure

(Fig. 1). Other membrane components, such as minor glycoproteins and macroglycolipids, probably also are present, and in principle could contribute to the inhibition. However, because band 3 is the major component and liposomes are effective at low concentrations, a reasonable working hypothesis is that band 3 is the active component in these liposomes. The precise mechanism of inhibition by band 3 and glycophorin remains to be established. Explanations based on toxicity to parasites or alteration of erythrocyte membrane properties are unlikely, since controls with band 3 from a different species or with liposomes alone were much less effective. A plausible interpretation is that liposomes containing band 3 bind to surface sites on the parasites and thereby block their attachment to band 3 on the erythrocyte membrane.

Participation of band 3 in invasion is not surprising, since this cell-surface protein is present in 1 million copies per cell. Band 3 is the principal component of intramembrane particles visualized by freeze-fracture electron microscopy (8). Attachment of band 3 to merozoite surface components could explain the rearrangement of intramembrane particles into a ring surrounding a particle-free region that occurs at the junction between merozoite and erythrocyte membrane (12). Band 3 is attached on the cytoplasmic surface of the membrane to the spectrin-actin membrane cytoskeleton by linkage to ankyrin (13). Thus removal of band 3 from the particle-free zone (the site of merozoite entry) would also clear this region of the spectrin meshwork and allow penetration of the parasite.

Malarial parasites infect many vertebrate species, including reptiles, birds, and mammals. It is likely that different species share some fundamental features of the process of invasion. Band 3 has closely related homologues in these species and may represent a common receptor for all malarial strains. It is pertinent to note that band 3 has been implicated in invasion of rhesus monkey erythrocytes by *P. knowlesi* (7).

It will be important to identify the putative band 3 receptor of *P. falciparum* merozoites. Such a protein would be the logical target for vaccines against malaria.

VINCENT C. N. OKOYE*

VANN BENNETT

Department of Cell Biology and
Anatomy, Johns Hopkins
School of Medicine,
Baltimore, Maryland 21205

References and Notes

1. WHO Third Annu. Rep. (1979), pp. 1-32; L. Luzzato, *Blood* **54**, 961 (1979).
2. J. A. Dvorak, L. H. Miller, J. Johnson, J. Rabbege, *Science* **187**, 748 (1978); M. Aikawa, L. H. Miller, J. Johnson, J. Rabbege, *J. Cell Biol.* **77**, 72 (1978); L. H. Miller, M. Aikawa, J. Johnson, T. Shiroishi, *J. Exp. Med.* **149**, 172 (1979).
3. G. A. Butcher, G. H. Mitchel, S. Cohen, *Nature (London)* **244**, 40 (1973); L. H. Miller, et al., *J. Mol. Med.* **1**, 55 (1975); L. H. Miller, et al., *J. Exp. Med.* **138**, 1597 (1973); G. Pasvol et al., *Lancet* **1984-I**, 907 (1984).
4. L. H. Miller et al., *J. Exp. Med.* **146**, 277 (1977); G. Pasvol, J. Wainscoat, D. J. Weatherall, *Nature (London)* **297**, 64 (1981); R. Howard, J. Haynes, McGinniss, L. H. Miller, *Mol. Biochem. Parasitol.* **6**, 303 (1982).
5. M. Perkins, *J. Cell Biol.* **90**, 563 (1981); J. Deas and L. Lee, *Am. J. Trop. Med. Hyg.* **30**, 1164 (1981).
6. M. Friedman, T. Blankenberg, G. Sensabaugh, T. Tenforde, *J. Cell Biol.* **98**, 1672 (1984).
7. L. H. Miller et al., *J. Clin. Invest.* **72**, 1357 (1983).
8. J. Yu and D. Branton, *Proc. Natl. Acad. Sci. U.S.A.* **73**, 389 (1976).
9. J. D. Haynes et al., *Nature (London)* **263**, 767 (1976).
10. C. Lambros and J. P. Vandenberg, *J. Parasitol.* **65**, 418 (1979).
11. V. Bennett, *Methods Enzymol.* **96**, 313 (1983); G. Fairbanks, T. L. Steck, D. F. H. Wallach, *Biochemistry* **10**, 2607 (1971); R. Flores, *Anal. Biochem.* **88**, 605 (1978).
12. M. Aikawa, L. H. Miller, J. Johnson, J. Rabbege, *J. Cell Biol.* **77**, 72 (1978).
13. V. Bennett and P. Stenbuck, *J. Biol. Chem.* **254**, 2533 (1979); *Nature (London)* **280**, 468 (1979).
14. Supported in part by grants from NIH (R01 AM29808 and K04 AM00926), the Army (DAMD-17-83-3209), and the MacArthur Foundation. We are grateful to D. Haynes for providing cultures of *P. falciparum* and to L. Miller for helpful and informative discussions. V.C.N.O. was supported by a grant from the World Health Organization.

* Present address: Department of Hematology, College of Medicine, University of Ibadan, Ibadan, Nigeria.

20 August 1984; accepted 5 October 1984

Human Erythrocyte Clathrin and Clathrin-uncoating Protein*

(Received for publication, June 4, 1985)

Jonathan Q. Davis and Vann Bennett‡

From the Department of Cell Biology and Anatomy, The Johns Hopkins School of Medicine, Baltimore, Maryland 21205

Clathrin, a $M_r = 72,000$ clathrin-associated protein, and myosin were purified in milligram quantities from the same erythrocyte hemolysate fraction. Erythrocyte clathrin closely resembled brain clathrin in several respects: (a) both are triskelions as visualized by electron microscopy with arms 40 nm in length with globular ends and a flexible hinge region in the middle of each arm, and these triskelions assemble into polyhedral "cages" at appropriate pH and ionic strength; (b) both molecules contain heavy chains of $M_r = 170,000$ that are indistinguishable by two-dimensional maps of ^{125}I -labeled peptides; and (c) both molecules contain light chains of $M_r \sim 40,000$ in a 1:1 molar ratio with the heavy chain. Erythrocyte clathrin is not identical to brain clathrin since antibody raised against the erythrocyte protein reacts better with erythrocyte clathrin than with brain clathrin and since brain clathrin contains two light chains resolved on sodium dodecyl sulfate gels while the light chain of erythrocyte clathrin migrates as a single band. The erythrocyte $M_r = 72,000$ clathrin-associated protein is closely related to a protein in brain that mediates ATP-dependent disassembly of clathrin from coated vesicles and binds tightly to clathrin triskelions (Schlossman, D. M., Schmid, S. L., Braell, W. A., and Rothman, J. E. (1984) *J. Cell Biol.* 99, 723-733). The erythrocyte and brain proteins have identical M_r on sodium dodecyl sulfate gels and identical maps of ^{125}I -labeled peptides, share antigenic sites, and bind tightly to ATP immobilized on agarose. Clathrin and the uncoating protein are not restricted to reticulocytes since equivalent amounts of these proteins are present in whole erythrocyte populations and reticulocyte-depleted erythrocytes. Clathrin is present at 6,000 triskelions/cell, while the uncoating protein is in substantial excess at 250,000 copies/cell.

Clathrin is a large, extended protein found in most eukaryotic cells that is a three-armed trimer (triskelion) containing three heavy chains of $M_r = 170,000$ and three light chains of $M_r = 30,000$ - $40,000$ (Ungewickell and Branton, 1981; Kirchhausen and Harrison, 1981). Clathrin triskelions form the coats of endocytic vesicles which are involved in receptor-mediated uptake of molecules into cells, as well as transfer of membrane proteins between Golgi, endoplasmic reticulum, and the plasma membrane (reviewed by Pearse and Bretscher,

1981). Clathrin undergoes reversible self-assembly reactions, forming coated pits on the plasma membrane which are precursors of coated vesicles that in turn lose their clathrin to a soluble pool of clathrin that can cycle back to the plasma membrane. Recently, a $M_r \sim 70,000$ protein has been purified from brain cytosol that disassembles clathrin coats to triskelions in an ATP-dependent manner and has been termed as "uncoating ATPase" (Schlossman *et al.*, 1984; Braell *et al.*, 1984; Schmid *et al.*, 1984). The uncoating protein presumably allows clathrin triskelions to recycle back to coated pits for another round of endocytosis. Little is known about the interactions of clathrin with membrane proteins and receptors. Clathrin will reassociate *in vitro* with protease-sensitive sites on clathrin-depleted coated vesicles, although the protein(s) responsible for this interaction have not been conclusively demonstrated (Unanue *et al.*, 1981). This report describes identification and purification of clathrin and the uncoating protein from the cytosol of human erythrocytes. These simple cells have the best understood plasma membrane in terms of the organization of its structural proteins. Proteins closely related to membrane skeletal components of erythrocytes such as spectrin, ankyrin, protein 4.1 (synapsin), and the anion transporter have been found in many other cell types (reviewed by Bennett, 1985). Moreover, proteins of other cells have been found in erythrocytes, including insulin receptors (Gambhir *et al.*, 1978; Grigorescu *et al.*, 1983), tropomyosin (Fowler and Bennett, 1984), and myosin (Fowler *et al.*, 1985). The well-characterized erythrocyte membrane thus may provide an excellent model system for elucidating the protein associations involved in clathrin-membrane interactions and endocytosis of receptor molecules.

EXPERIMENTAL PROCEDURES

Materials— Na^{125}I was from Amersham Corp. Hydroxylapatite (high resolution) was from Calbiochem-Behring. Plastic thin-layer sheets coated with 0.1 mm of cellulose was from Merck. Diisopropyl fluorophosphate, phenylmethylsulfonyl fluoride, dithiothreitol (DTT), and ATP-agarose (linked through C-8) were from Sigma. Nitrocellulose paper and electrophoresis reagents were from Bio-Rad. Sucrose and ammonium sulfate were from Schwarz/Mann. α -Chymotrypsin (44 units/mg) was from Worthington. Cyanogen bromide-activated Sepharose 4B, dextran 500, Protein A, Protein A-Sepharose, Percoll, and Sephacryl S-400 were from Pharmacia. DEAE-53-cellulose was from Whatman. Erythrocyte ghosts were prepared as described (Bennett, 1983). Bovine brains were obtained within 30 min of death from a local slaughterhouse; tissue from the cerebral cortex was washed with 0.32 M sucrose and frozen in liquid nitrogen. Frozen brain was stored at -100°C and used within 6 weeks.

Methods—Brain tissue was homogenized with a Brinkmann Instruments Polytron (large head) for 30-60 s at a setting of 5.5. SDS-polyacrylamide electrophoresis was performed on 3.5-17% exponential gradient slab gels with the buffers of Fairbanks *et al.* (1971). Immunoblot analysis was performed by electrophoretically transfer-

* This research was supported by National Institutes of Health Grants R01 AM19808, R01 GM33996, and RCDA K04 AM00926 and Grant DAMD17-83-C-3209 from the United States Army. The costs of publication of this article were defrayed in part by the payment of page charges. This article must therefore be hereby marked "advertisement" in accordance with 18 U.S.C. Section 1734 solely to indicate this fact.

‡ To whom correspondence should be addressed.

¹ The abbreviations used are: DTT, dithiothreitol; SDS, sodium dodecyl sulfate; EGTA, ethylene glycol bis(β -aminoethyl ether)-N,N,N',N'-tetraacetic acid.

ring proteins from SDS gels to nitrocellulose paper (Towbin *et al.*, 1979) using conditions as described (Bennett and Davis, 1981). Protein was determined by the method of Bradford (1976) or Lowry *et al.* (1951) or by absorbance at 280 nm. The concentration of purified uncoating protein was determined by the method of Bradford (Schlossman *et al.*, 1984), and scans of Coomassie Blue-stained gels were used to determine the purity. The concentration of erythrocyte clathrin was determined by absorbance at 280 nm using an $E_{280\text{ nm}}$ of 11.9 (Unanue *et al.*, 1981) and by scans of stained gels to determine the amount of clathrin heavy chain relative to total protein. Autoradiography was performed at -100°C with X-Omat AR film (Kodak) and Cronex intensifier screens (DuPont). Proteins were radioiodinated with Na^{125}I using chloramine T as an oxidant (Hunter and Greenwood, 1962).

Erythrocytes were isolated from freshly drawn blood (4 units) and depleted of other cell types as described (Bennett, 1983). The cells were lysed in 10 volumes of 7.5 mM sodium phosphate buffer, pH 7.4, 1 mM NaEGTA, 0.01% (v/v) diisopropyl fluorophosphate and then concentrated and washed on a Millipore filtration apparatus with a Pellicon cassette system, using a Durapore 0.5- μ filter. The initial 6 liters of hemolysate was collected and used for the starting material for purification of clathrin, myosin, and uncoating protein.

Two-dimensional maps of ^{125}I -labeled α -chymotryptic peptides were performed by modification of the procedure of Elder *et al.* (1977). Samples were electrophoresed on 3.5–17% exponential gradient slab gels with the buffers of Fairbanks *et al.* (1971). The gels were lightly stained with Coomassie Blue, and the protein band was excised, destained completely, and equilibrated in 10 mM phosphate buffer, pH 7.4. The gel slices were dehydrated in an 80°C oven and then iodinated with 0.5 mCi of Na^{125}I in a 200- μ l final volume containing 50 mM phosphate buffer, pH 7.4, 0.1% SDS, 200 $\mu\text{g}/\text{ml}$ chloramine T for 1 h at room temperature. The reaction was stopped by addition of 20 μ l of DTT (10 mg/ml), and the gel slices were washed extensively over a period of days with multiple changes of buffer until the counts in the supernatants were less than 5% of the total. The slices were then equilibrated with 50 mM ammonium acetate, 1 mM sodium azide, pH 7.0, suspended in 0.5 ml of buffer, and digested for 20 h at 37°C with two additions of 25 μg of α -chymotrypsin. The digest was lyophilized and peptide maps were prepared.

Antisera were raised in three New Zealand White rabbits, which were injected subcutaneously with 1–200 μg of erythrocyte clathrin as purified in Fig. 1, in complete Freund's adjuvant, followed by four similar injections at 2-week intervals with antigen in incomplete adjuvant. Titer was monitored by the immunoblot method (see above) and was maximal after four injections. Pooled immune sera were diluted with 1 volume of 0.15 M NaCl, 10 mM sodium phosphate, pH 7.4, 1 mM NaEDTA, 1 mM NaN_3 , 0.2% (v/v) Triton X-100 and heated to 60°C in the presence of 200 $\mu\text{g}/\text{ml}$ phenylmethylsulfonyl fluoride to minimize protease activity. Antibody against erythrocyte clathrin-uncoating protein and clathrin was isolated by affinity chromatography using purified proteins (Figs. 1 and 3) coupled to cyanogen bromide-activated Sepharose CL-4B ($\sim 600\text{ }\mu\text{g}$ of protein/ml of agarose). 100 ml of diluted serum was applied to a 5-ml column of uncoating protein-Sepharose at 4°C with a flow rate of 10 ml/h. The breakthrough was then applied to a 5-ml column of erythrocyte clathrin-Sepharose. Both columns were washed successively with 100 ml of 0.5 M NaCl, 10 mM sodium phosphate, pH 7.4, 0.2% Triton X-100, 1 mM NaN_3 , 50 ml of 2 M urea, 0.1 M glycine, 0.1% Triton X-100, and 20 mM Na acetate, pH 5.0 until the A_{280} dropped to 0. The antibodies were then eluted with 0.1 M glycine HCl, pH 2.2, into tubes containing 0.1 ml of Tris base/ml of fractions collected. Peak fractions were dialyzed against 0.15 M NaCl, 10 mM sodium phosphate, pH 7.4, 1 mM NaN_3 , 10% sucrose and stored at -70°C . Preimmune antibody was purified from pooled preimmune serum by affinity chromatography on Protein A-Sepharose CL-4B employing the same washes and elution conditions.

Amounts of erythrocyte clathrin and uncoating protein were estimated in red blood cells by dissolving packed cells (cell number determined by counting in a hemocytometer) in 10 volumes of $2\times$ concentrated SDS-polyacrylamide gel electrophoresis buffer, and 10- or 20- μ l samples of erythrocytes or known amounts of pure clathrin and uncoating protein were run on gels in triplicate. The proteins were then electrophoretically transferred to nitrocellulose, incubated overnight with 2 $\mu\text{g}/\text{ml}$ affinity-purified antibodies and then labeled for 2 h with ^{125}I -Protein A ($2\times 10^6\text{ cpm}/\text{ml}$) and stained lightly with 0.2% Ponceau S in 3% trichloroacetic acid, and the appropriate bands were cut out and counted in a γ -counter. Background was determined using gel lanes lacking protein.

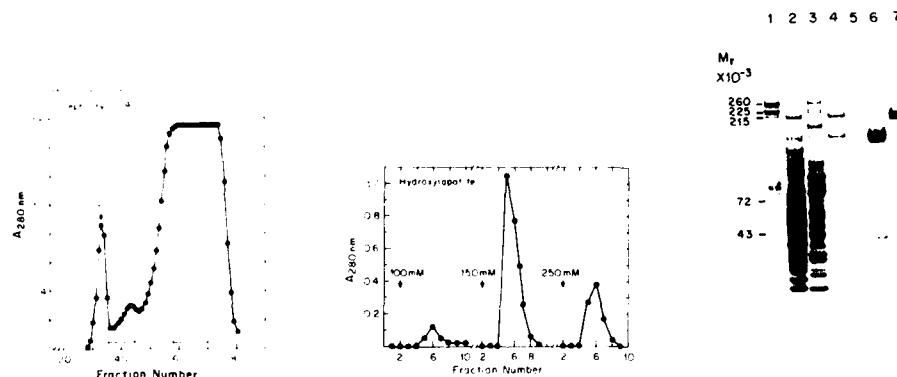


FIG. 1. Purification of human erythrocyte clathrin and myosin from a low salt hemolysate fraction by chromatography on DEAE-cellulose, Sepharose S-400, and hydroxylapatite. Human red blood cell hemolysate (6 liters) (see "Methods") was adjusted to 50 mM final concentration in sodium chloride and batchwise adsorbed with 120 ml of DEAE-53-cellulose previously equilibrated in 7.5 mM sodium phosphate buffer, 1 mM NaEDTA, 1 mM sodium azide, pH 7.4. The DEAE-cellulose was collected on a glass-centered funnel and washed with 2 liter of cold lysis buffer with the addition of 100 mM sodium chloride and then poured into a column and eluted at 20 ml/h with 200 mM NaCl dissolved in lysis buffer, collecting 15-ml fractions. Protein was monitored by polyacrylamide gel electrophoresis, and $M_r = 170,000$ material was pooled. Solid ammonium sulfate was added to the pooled DEAE fractions to 60% saturation and left on ice for 1 h, and precipitated protein was collected by centrifugation at $30,000\times g$ for 30 min. The pellet was resuspended in 9 ml of 1 M NaBr, 1 mM NaEDTA, 10 mM phosphate buffer, pH 7.4, 0.5 mM DTT, 1 mM azide (column buffer), centrifuged at $100,000\times g$ for 30 min, applied to a Sepharose S-400 column (2.5 \times 85 cm) equilibrated in the same buffer, and run at a flow rate of 20 ml/h with 5-ml fractions (left panel). The clathrin/myosin peak was pooled, adjusted to 2 mM MgCl_2 , and applied to a hydroxylapatite column (5 ml) equilibrated in column buffer without NaEDTA. The hydroxylapatite was eluted with the same buffer with increasing sodium phosphate concentrations of 50, 100, 150, and 250 mM at pH 7.4 (middle panel). Samples were analyzed by electrophoresis on a SDS-polyacrylamide gel stained with Coomassie Blue (right panel). Lane 1, human erythrocyte ghosts; lane 2, DEAE-200 mM sodium chloride elution; lane 3, DEAE-500 mM sodium chloride elution; lane 4, Sepharose S-400 pool; lane 5, hydroxylapatite-100 mM phosphate elution; lane 6, purified clathrin from the hydroxylapatite column (150 mM elution); lane 7, purified myosin from the hydroxylapatite column (250 mM elution).

Dense older erythrocytes were isolated on Percoll density gradients to determine if older cells contained similar amounts of clathrin and uncoating protein as starting cells. Percoll was made isotonic with NaCl and then diluted with 0.15 M saline to the following densities, 1.09, 1.1, 1.105, 1.11, 1.115, and 1.120, and layered in steps (1.5 ml each) in 15-ml centrifuge tubes. Aliquots of starting cells were taken, and identical samples (2–5 ml) were layered onto the gradients and centrifuged in a Beckman JA-20 rotor at 12,000 rpm for 15 min. The erythrocytes were distributed in multiple density bands. The upper 50% of the total erythrocytes were aspirated off, and the remaining cells were washed and packed to the same cell density as the starting cells. Starting and Percoll isolated cells were then dissolved in 10 volumes of $2 \times$ SDS-polyacrylamide gel electrophoresis buffer and run on gels, and an immunoblot analysis was performed.

RESULTS

Identification and Purification of Erythrocyte Clathrin—Erythrocyte clathrin triskelions were initially discovered by electron microscopy as contaminants in preparations of myosin isolated from erythrocyte cytosol (Fowler *et al.*, 1985). Clathrin was purified from erythrocyte cytosol using the following steps, which were monitored by SDS gels: 1) batch adsorption to DEAE-cellulose and elution with a step gradient, 2) precipitation with ammonium sulfate, 3) gel filtration on Sephacryl S-400 in 1 M sodium bromide, and 4) hydroxylapatite chromatography (Fig. 1). This procedure also yields erythrocyte myosin in higher purity and yield than reported previously (Fowler *et al.*, 1985). The isolated clathrin contained polypeptides of $M_r = 170,000$ and $41,000$ in approximately a 1:1 molar stoichiometry that comprised about 90% of the Coomassie Blue staining material on SDS gels. Two polypeptides of $M_r = 72,000$ and $71,000$ copurified with the $M_r = 170,000$ and $41,000$ polypeptides and may be associated with clathrin (see below). The recovery of clathrin from 700 ml of packed erythrocytes was 3.3 mg, while 2.4 mg of myosin was isolated.

Erythrocyte clathrin visualized in the electron microscope following rotary shadowing with platinum is a three-armed structure (Fig. 2) identical to published images of brain clathrin which were termed triskelions (Ungewickell and Branton, 1981; Kirchhausen and Harrison, 1981). Each arm of erythrocyte clathrin triskelions is about 40 nm in length, and has a bend or kink approximately in the mid-region, and has a globular knob on the end, as reported for brain clathrin (Ungewickell and Branton, 1981; Kirchhausen and Harrison, 1981, 1984). As expected from experience with other clathrins, erythrocyte clathrin triskelions will assemble into polyhedral "cages" approximately 120 nm in diameter when dialyzed against low ionic strength buffers at pH 6.5 or less (Fig. 2).

Erythrocyte clathrin heavy chain and brain clathrin heavy chain are closely related in amino acid sequence, since the $M_r = 170,000$ polypeptides of brain and erythrocyte clathrin produce identical two-dimensional ^{125}I -labeled peptide maps (Fig. 3). The brain and erythrocyte clathrin heavy chains are not identical in sequence, however, since antibody raised against erythrocyte clathrin cross-reacts about 2-fold better with erythrocyte clathrin than with brain clathrin by immunoblots (not shown). Presumably, the erythrocyte antibody recognizes erythrocyte-specific determinants that are not labeled with ^{125}I or which happen to co-migrate on peptide maps.

Erythrocyte clathrin and brain clathrin differ in their light chains. The brain protein contains two polypeptides with an apparent M_r of 41,000 and 43,000 present in a 1:2 molar ratio, as noted previously (Ungewickell and Branton, 1981; Kirchhausen and Harrison, 1981). The apparent M_r of brain clathrin light chains is higher than values of 33,000 and 36,000 reported by other investigators, but this difference is due to

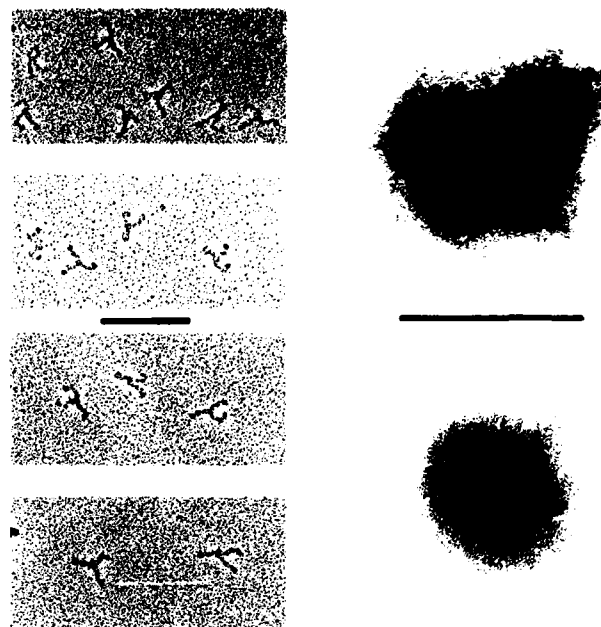


FIG. 2. Visualization of erythrocyte clathrin by electron microscopy. Erythrocyte clathrin (660 $\mu\text{g}/\text{ml}$) was diluted to 10 $\mu\text{g}/\text{ml}$ with 100 mM ammonium formate, pH 7.0, 30% (v/v) glycerol, 1 mM sodium azide, sprayed onto freshly cleaved mica, dried under vacuum at room temperature, and rotary-shadowed with platinum at an angle of 6° followed by carbon (Shotton *et al.*, 1979) (left panel). Clathrin baskets were formed by dialysis into 20 mM sodium phosphate buffer, 1 mM MgCl_2 , 1 mM NaEGTA, 0.5 mM DTT, 1 mM sodium azide, pH 6.6 overnight and then applied to Formvar-coated grids and stained with 1% uranyl acetate (right panel). Bar = 200 nm.

use of different buffers in electrophoresis. Erythrocyte clathrin contains a single light chain that co-migrates with the lower M_r light chain of brain clathrin (Fig. 3). It is possible that erythrocyte clathrin contains distinct light chains that co-migrate on SDS gels or that in the erythrocyte system one of the light chains has been lost.

The amount of clathrin in erythrocytes was estimated at 6000 triskelions/cell by quantitative immunoblots (Table I). Clathrin is present in cells other than reticulocytes, since erythrocytes depleted of reticulocytes by fractionation on Percoll gradients had equivalent amounts of clathrin as unfractionated erythrocytes (Table I). Clathrin thus is not lost during maturation of erythrocytes. The amount of clathrin per erythrocyte is about 20% of the number of copies per rat lymphocyte, which are cells of comparable size to erythrocytes (Goud *et al.*, 1985).

Purification of the $M_r = 72,000$ Clathrin-uncoating Protein from Erythrocyte Cytosol—Brain clathrin baskets have recently been reported to be disassembled in an ATP-dependent reaction involving a protein of $M_r \sim 70,000$ that binds to ATP affinity columns and has been termed an uncoating ATPase (Schlossman *et al.*, 1984; Braell *et al.*, 1984; Schmid *et al.*, 1984). A protein closely related to the brain uncoating ATPase is present in erythrocyte cytosol and has been purified by affinity chromatography with an ATP-Sepharose column (Fig. 4). The isolated erythrocyte $M_r = 72,000$ polypeptide was 81% pure based on scans of Coomassie Blue-stained gels, and about 7 mg was recovered from 700 ml of packed erythrocytes. The $M_r = 72,000$ protein from cytosol is identical to the $M_r = 72,000$ polypeptide that copurified with erythrocyte clathrin since two-dimensional peptide maps of these proteins are very similar (Fig. 5). The $M_r = 71,000$ polypeptide copu-

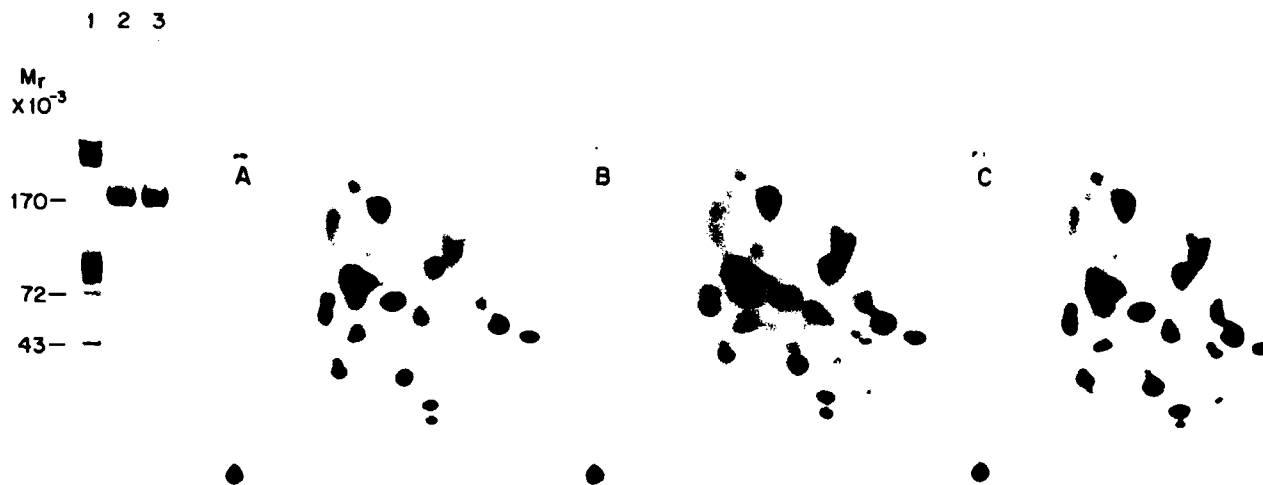


FIG. 3. The heavy chains of erythrocyte clathrin and brain clathrin have identical two-dimensional peptide maps of ^{125}I -labeled chymotryptic peptides. Maps are (right panel): erythrocyte clathrin heavy chain (A), brain clathrin heavy chain (B), and a mixture of peptides from A and B (C). See "Methods" for experimental procedures. Erythrocyte clathrin was isolated as described in the legend to Fig. 1, and brain clathrin was purified as described by Ungewickell and Branton (1981) except that the second gel filtration step in triethanolamine was omitted. Left panel, SDS-polyacrylamide gels stained with Coomassie Blue: lane 1, erythrocyte ghost membranes; lane 2, brain clathrin; lane 3, erythrocyte clathrin.

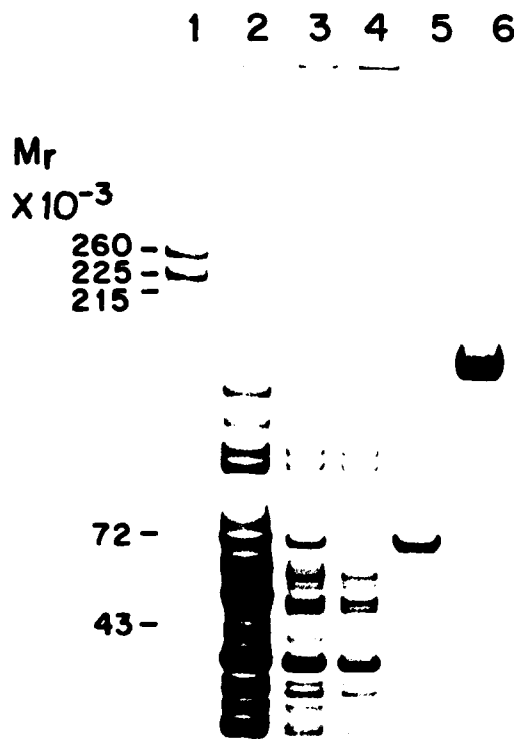


FIG. 4. Purification of a $M_r = 72,000$ erythrocyte clathrin-associated protein from hemolysate by chromatography on DEAE-cellulose, Sephacryl S-400, hydroxylapatite, and an ATP-agarose affinity column. Immune sera against the isolated clathrin which contained antibodies against protein migrating on gels at $M_r = 70,000$ and $72,000$ (see Fig. 6) were used to screen fractions by immunoblot analysis (see "Methods") of the clathrin purification (Fig. 1). A large pool of cross-reactivity was found in the DEAE-200 mM eluate which migrated at the Sephacryl S-400 column toward the

TABLE I

Quantitation of clathrin and uncoating protein in erythrocytes

	Erythrocyte clathrin (triskelions)	Uncoating protein (monomer)
	molecules/cell	
Unfractionated erythrocytes ^a	6,050 \pm 139	257,690 \pm 10,800
Reticulocyte-depleted erythrocytes ^b	6,460 \pm 174	264,650 \pm 7,940

^a Determined by a quantitative immunoblotting procedure as described under "Experimental Procedures." Molecule numbers were determined by (calculated mol of protein/cell number (determined by direct counting in a hemocytometer)) $\times 6.03 \times 10^{23}$. Values were an average of triplicate samples.

^b Determined in a separate experiment with control cells and dense cells isolated on Percoll gradients (see "Experimental Procedures"). Molecule numbers were extrapolated from a per cent of control cells in the same assay, using numbers generated in the above quantitation assay for molecules per control cells. Values were an average of duplicate samples.

ryfying with clathrin has distinct maps and may be another unidentified clathrin-associated protein. Band 4.2, a membrane protein of $M_r = 72,000$, also exhibited a distinct peptide map (Fig. 5).

The human erythrocyte $M_r = 72,000$ clathrin-associated protein is closely related to the uncoating ATPase of bovine

included volume (Fig. 1). The Sephacryl S-400 fractions were pooled (see Fig. 1), adjusted to 1 mM MgCl_2 , and applied to a hydroxylapatite column (20 ml) in the presence of 1 M sodium bromide. The cross-reacting polypeptide did not adsorb to the column, and this unadsorbed material was then dialyzed against 10 mM sodium phosphate buffer, 25 mM KCl, 0.5 mM DTT, 1 mM sodium azide, 2 mM MgCl_2 , pH 7.4. The dialysate was applied to an ATP-agarose column (10 ml, 0.8×13 cm), which was washed until the $A_{280\text{ nm}}$ approached zero, and then eluted with 20 volumes of buffer with 2 mM ATP at 10 ml/h. The ATP column eluate was collected on a 4-ml DEAE-53 column which was then eluted with 0.5 M sodium chloride. Samples were analyzed by electrophoresis on a SDS-polyacrylamide gel stained with Coomassie Blue. Lane 1, human erythrocyte ghosts; lane 2, Sephacryl S-400 pool; lane 3, ATP-agarose start; lane 4, ATP-agarose breakthrough; lane 5, purified erythrocyte clathrin-associated protein from the DEAE-0.5 M sodium chloride elution; lane 6, erythrocyte clathrin.



FIG. 5. Two-dimensional peptide maps of ^{125}I -labeled peptides from purified erythrocyte clathrin-associated protein (A), Band 4.2 of erythrocyte membranes (B), the $M_r = 72,000$ contaminant in the isolated clathrin (C), and the $M_r = 71,000$ contaminant in the isolated clathrin (D). See "Methods" for experimental procedures. The clathrin-associated proteins were isolated as described in the legend to Fig. 1.

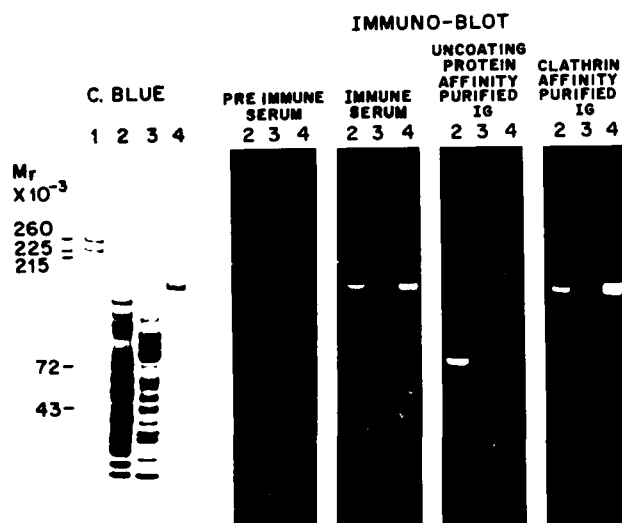


FIG. 6. Characterization of affinity-purified antibody against erythrocyte clathrin and clathrin-uncoating protein by immunoblot analysis. Immune sera which contained antibodies against clathrin heavy chain as well as the $M_r = 72,000$ clathrin-associated protein were applied to affinity columns in series containing first a clathrin-associated protein-Sepharose column followed by the clathrin-Sepharose affinity column (see "Methods"). Gels were stained with Coomassie Blue (C. BLUE) (left panel) or electrophoretically transferred to nitrocellulose paper for immunoblot analysis (see "Methods" (right panels)). Lane 1, human erythrocyte ghosts; lane 2, DEAE-0.2 M NaCl elution from the clathrin purification (Fig. 1); lane 3, DEAE-0.5 M NaCl elution from the clathrin purification; lane 4, purified erythrocyte clathrin.

brain based on cross-reactivity (Fig. 7) and peptide maps (Fig. 8). Antibody against the erythrocyte protein was isolated by affinity chromatography using immobilized cytosolic protein from antisera raised against erythrocyte clathrin and its associated proteins (Fig. 6). The affinity-purified antibody against the erythrocyte $M_r = 72,000$ protein cross-reacted with a $M_r = 72,000$ polypeptide present in brain membranes and brain cytosol (Fig. 7). The cross-reacting $M_r = 72,000$ polypeptide of brain cytosol was purified by affinity chromatography on an ATP-Sepharose column using the procedure described for the uncoating ATPase (Schlossman *et al.*, 1984) (Fig. 7). The antibody also cross-reacted with a polypeptide of $M_r = 110,000$, but this protein did not bind to the ATP affinity column (Fig. 7) and exhibited distinct peptide maps (not shown). The erythrocyte $M_r = 72,000$ protein is identical or closely related in amino acid sequence to the cross-reacting $M_r = 72,000$ protein from brain since peptide maps of these proteins were indistinguishable (Fig. 8). The erythrocyte $M_r = 72,000$ protein also was capable, in preliminary studies, of

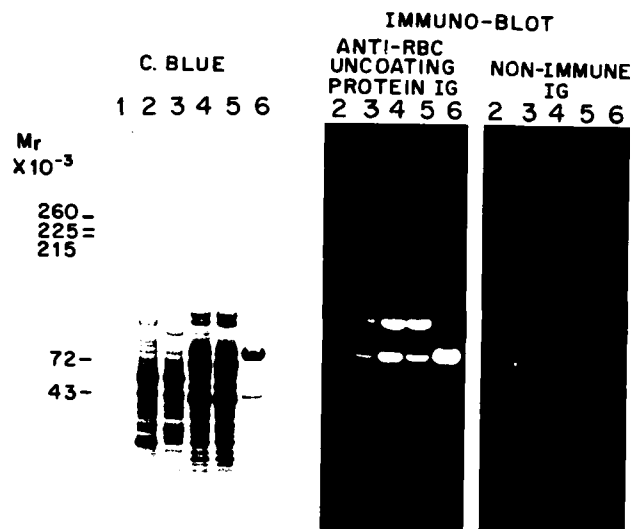


FIG. 7. An immunoreactive form of the erythrocyte $M_r = 72,000$ clathrin-associated protein is present in brain membranes and brain cytosol and copurifies with brain clathrin-uncoating protein. Brain clathrin-uncoating protein was partially purified from brain cytosol by a modification of the procedure of Schlossman *et al.* (1984). 300 g of bovine brain was homogenized in 1.5 liters of 0.32 M sucrose, 2 mM NaEGTA, pH 7.4 (see "Methods"). Brain cytosol was prepared from a post-nuclear $30,000 \times g$ supernatant by a final $100,000 \times g$ centrifugation for 90 min. Cytosol was applied to a 60-ml DEAE-53 column (2.5×13 cm) equilibrated with 10 mM sodium phosphate, 1 mM NaEDTA, 1 mM NaN_3 , pH 7.4, at 30 ml/h. The column was washed and then eluted with salt cuts of 50, 150, and 250 mM sodium chloride dissolved in equilibration buffer. The 150 mM elution which contained the cross-reacting material was pooled and then resuspended in 10 mM sodium phosphate, 25 mM KCl, 0.5 mM DTT, 1 mM NaEDTA, 1 mM NaN_3 , pH 7.4, and dialyzed against 2×4 liters of the same buffer, the latter lacking EDTA. The dialysate was adjusted to 1 mM MgCl_2 and applied to a 10-ml ATP-agarose column (0.8×13 cm) at 20 ml/h. The column was washed and then eluted with 20 volumes of buffer with 1 mM ATP, and the eluted material was collected on a 5-ml DEAE-53 column which was eluted with 0.5 M NaCl. Samples were run on SDS gels and stained with Coomassie Blue (C. BLUE) (left panel) or electrophoretically transferred to nitrocellulose paper incubated with either affinity-purified Ig against erythrocyte $M_r = 72,000$ protein or nonimmune Ig for immunoblot analysis (see "Methods" (right panels)). Lane 1, erythrocyte ghosts; lane 2, demyelinated, washed brain membranes; lane 3, brain cytosol; lane 4, ATP-agarose starting material; lane 5, ATP-agarose breakthrough; lane 6, partially purified brain clathrin-uncoating protein from the DEAE catcher column.



FIG. 8. Two-dimensional peptide maps of ^{125}I -labeled peptides from the $M_r = 72,000$ clathrin-associated protein from erythrocytes (A), the brain clathrin-uncoating protein (B), and a mixture of peptides from A and B (C). See "Methods" for experimental procedures. The erythrocyte protein was purified as described in the legend to Fig. 4, and the brain protein as described in the legend to Fig. 7.

promoting disassembly of clathrin cages from brain using the procedures of Schlossman *et al.* (1984) (data not shown). It appears that both clathrin and the uncoating ATPase are highly conserved proteins with very similar forms in human erythrocytes and bovine brain.

The amounts of erythrocyte clathrin-uncoating protein in cytosol are surprisingly high and were estimated at about 250,000 copies/cell (Table I). As is the case with clathrin, erythrocytes depleted of reticulocytes had unaltered amounts of uncoating protein (Table I). At least 90% of the uncoating protein is cytosolic, although some can be detected in washed membranes by immunoblots (not shown). Band 4.2 is a major membrane protein of identical mobility in SDS gels, but peptide maps of Band 4.2 and the uncoating protein indicate that these polypeptides are unrelated (Fig. 5).

DISCUSSION

This report describes identification and purification of clathrin and a $M_r = 72,000$ clathrin-associated protein from the cytosol of mature human erythrocytes. Erythrocyte clathrin closely resembles brain clathrin in several respects: (a) both are triskelions as visualized by electron microscopy with arms ~ 40 nm in length with a globular end and hinge region in the middle of each arm, and these triskelions will assemble into polyhedral cages at appropriate pH and ionic strength; (b) both molecules contain heavy chains of $M_r = 170,000$ that are indistinguishable by two-dimensional peptide maps; and (c) both molecules contain light chains in a 1:1 molar ratio with the heavy chain, although brain clathrin has two forms of light chain, while erythrocyte clathrin may have only one form of light chain. Erythrocyte $M_r = 72,000$ clathrin-associated protein is closely related or identical to a protein recently discovered in brain that mediates ATP-dependent disassembly of clathrin from coated vesicles and binds tightly to clathrin triskelions (Schlossman *et al.*, 1984). The erythrocyte and brain proteins have identical M_r on SDS gels and identical two-dimensional peptide maps, share antigenic sites, and are purified by affinity chromatography on ATP-agarose. The clathrin and uncoating protein are not restricted to reticulocytes and are present in equivalent amounts in whole erythrocyte populations and reticulocyte-depleted erythrocytes (Table I).

The presence of clathrin in erythrocytes at some stage of development should have been expected since these cells are very active as reticulocytes in endocytosis of iron-transferrin complexes for the synthesis of hemoglobin (Hemmaplardh

and Morgan, 1977; Jandl and Katz, 1963). Clathrin-coated vesicles presumably engaged in endocytosis of transferrin-receptor complexes have been visualized in reticulocytes and are observed budding from the inner surface of the membrane at sites free of spectrin (Harding *et al.*, 1983). Furthermore, insulin receptors in human erythrocytes are reversibly down-regulated in the presence of insulin (Peterson *et al.*, 1983), and in other cells such down-regulation has been linked to a clathrin-mediated endocytosis.

Mammalian erythrocytes lose their transferrin receptors within several days of entering the circulation, with a reduction from about 400,000 to less than 10,000 receptors/cell (Van Bockxmeer and Morgan, 1979; Frazier *et al.*, 1982; Enns *et al.*, 1981; Pan and Johnstone, 1983). Furthermore, insulin receptors also are enriched in younger erythrocytes and are lost during *in vivo* aging of erythrocytes (Eng *et al.*, 1980; Dons *et al.*, 1981). It therefore is likely that the 6,000 clathrin triskelions of a mature erythrocyte are remnants from a more active period in erythrocyte development. Assembly of these triskelions into coated vesicles may be unfavored since erythrocytes contain large amounts of the uncoating protein. An activity of residual clathrin in maintenance level endocytosis of receptors for transferrin, insulin, and possibly other ligands cannot be excluded at this point, however.

The erythrocyte uncoating protein is present at 250,000 copies/cell or 40-fold excess over clathrin and is a significant component of erythrocyte cytosol. The uncoating protein in brain, in contrast, is present in approximately equivalent amounts to clathrin triskelions (Schlossman *et al.*, 1984). The large excess of erythrocyte uncoating protein over clathrin could be explained by different rates of degradation of these proteins. Another possibility is that the uncoating protein has additional functions besides disassembly of clathrin coats. For example, the uncoating protein could be involved in the dramatic loss of transferrin receptors from reticulocytes. These receptors are spontaneously shed from erythrocytes in vesicles containing the transferrin receptor and an unidentified polypeptide of $M_r = 72,000$ (Pan and Johnstone, 1983). It will be important to determine if the $M_r = 72,000$ polypeptide in receptor-containing vesicles is the uncoating protein and if the uncoating protein can associate directly with the transferrin receptor. It also will be of interest to determine when in erythrocyte development the uncoating protein is synthesized and if its synthesis correlates with the loss of transferrin receptors.

The presence in erythrocytes of clathrin and at least one

protein known to interact with clathrin suggests that other components of the coated vesicle may also be found in these cells. Likely candidates would be polypeptides of $M_r = 100,000$ and $110,000$ that may be involved in linkage of clathrin to vesicle membranes in brain (Unanue *et al.*, 1981) and in assembly of clathrin into cages (Zaremba and Keene, 1983). If these proteins, or at least their membrane-binding sites, are in erythrocytes, it should be possible to elucidate in this simple system how clathrin interacts with integral membrane proteins such as receptors. Clathrin does not bind to inside-out vesicles from erythrocytes (Unanue *et al.*, 1981), although this negative result could be explained by extraction of clathrin-binding protein(s) during preparation of vesicles. The uncoating protein in brain is present in washed membranes as well as cytosol (Fig. 7) and may interact with membrane sites, in addition to clathrin, that can be identified and studied in erythrocytes. It is of interest in this regard that some of the erythrocyte uncoating protein remains associated with washed erythrocyte ghosts (not shown).

Acknowledgments—We thank Kevin Gardner for providing us with erythrocyte cytosol and Arlene Daniel for preparation of the manuscript.

REFERENCES

- Bennett, V. (1983) *Methods Enzymol.* **96**, 313-324
 Bennett, V. (1985) *Annu. Rev. Biochem.* **54**, 273-304
 Bennett, V., and Davis, J. (1981) *Proc. Natl. Acad. Sci. U. S. A.* **78**, 7550-7554
 Bradford, M. M. (1976) *Anal. Biochem.* **72**, 248
 Braell, W. A., Schlossman, D. M., Schmid, S. L., and Rothman, J. E. (1984) *J. Cell Biol.* **99**, 734-741
 Dons, R. F., Corash, L. M., and Gordon, P. (1981) *J. Biol. Chem.* **256**, 2982-2987
 Elder, J. H., Pickett, R. A., II, Hampton, J., and Lerner, R. A. (1977) *J. Biol. Chem.* **252**, 6510-6516
 Eng, J., Lee, L., and Yalow, R. S. (1980) *Diabetes* **29**, 164-166
 Enns, C. A., Shindelman, J. E., Tonik, S. E., and Sussman, H. H. (1981) *Proc. Natl. Acad. Sci. U. S. A.* **78**, 4222-4225
 Fairbanks, G., Steck, T. L., and Wallach, D. F. H. (1971) *Biochemistry* **10**, 2606-2617
 Fowler, V. M., and Bennett, V. (1984) *J. Biol. Chem.* **259**, 5978-5989
 Fowler, V. M., Davis, J., and Bennett, V. (1985) *J. Cell Biol.* **100**, 47-55
 Frazier, J. L., Caskey, J. H., Yoffe, M., and Seligman, P. A. (1982) *J. Clin. Invest.* **69**, 853-865
 Gambhir, K. K., Archer, J. A., and Bradley, C. J. (1978) *Diabetes* **27**, 701-708
 Goud, B., Huet, C., and Louvard, D. (1985) *J. Cell Biol.* **100**, 521-527
 Grigorescu, F., White, M., and Kahn, C. R. (1983) *J. Biol. Chem.* **258**, 13708-13716
 Harding, C., Heuser, J., and Stahl, P. (1983) *J. Cell Biol.* **97**, 329-339
 Hemmaplardh, P., and Morgan, E. H. (1977) *Br. J. Haematol.* **36**, 85-96
 Hunter, W., and Greenwood, F. (1962) *Nature* **194**, 495-496
 Jandl, J. H., and Katz, J. H. (1963) *J. Clin. Invest.* **42**, 314-326
 Kirchhausen, T., and Harrison, S. C. (1981) *Cell* **23**, 755-761
 Kirchhausen, T., and Harrison, S. C. (1984) *J. Cell Biol.* **99**, 1725-1734
 Lowry, O. H., Rosebrough, N. J., Farr, A. L., and Randall, R. J. (1951) *J. Biol. Chem.* **193**, 265-275
 Pan, B.-T., and Johnstone, R. M. (1983) *Cell* **33**, 967-977
 Pearse, B. M., and Bretscher, M. (1981) *Annu. Rev. Biochem.* **50**, 85-101
 Peterson, S. W., Miller, A. L., Kellerher, R. S., and Murray, E. F. (1983) *J. Biol. Chem.* **258**, 9605-9607
 Schlossman, D. M., Schmid, S. L., Braell, W. A., and Rothman, J. E. (1984) *J. Cell Biol.* **99**, 723-733
 Schmid, S. L., Braell, W. A., Schlossman, D. M., and Rothman, J. E. (1984) *Nature* **311**, 228-231
 Shotton, D. M., Burke, B. E., and Branton, D. (1979) *J. Mol. Biol.* **131**, 303-329
 Towbin, H., Staehelin, T., and Gordon, J. (1979) *Proc. Natl. Acad. Sci. U. S. A.* **76**, 4350-4354
 Unanue, E., Ungewickell, E., and Branton, D. (1981) *Cell* **26**, 439-446
 Ungewickell, E., and Branton, D. (1981) *Nature* **289**, 420-422
 Van Bockxmeer, F. M., and Morgan, E. H. (1979) *Biochim. Biophys. Acta* **584**, 76-83
 Zaremba, S., and Keene, J. H. (1983) *J. Cell Biol.* **97**, 1339-1347

A New Erythrocyte Membrane-associated Protein with Calmodulin Binding Activity

IDENTIFICATION AND PURIFICATION*

Kevin Gardner† and Vann Bennett

From the Department of Cell Biology and Anatomy, Johns Hopkins University School of Medicine, Baltimore, Maryland 21205

(Received for publication, July 17, 1985)

A new protein that binds calmodulin has been identified and purified to >95% homogeneity from the Triton X-100-insoluble residue of human erythrocyte ghost membranes (cytoskeletons) by DEAE chromatography and preparative rate zonal sucrose gradient sedimentation. This ghost calmodulin-binding protein is an α/β heterodimer with subunits of $M_r = 103,000$ (α) and $97,000$ (β). The protein exhibits a Stokes radius of 6.9 nm and a sedimentation coefficient of 6.8 S, corresponding to a molecular weight of 197,000. Moreover, the protein is cross-linked by Cu^{2+} /phenanthroline to a dimer of $M_r = 200,000$. The $M_r = 97,000$ β subunit was identified as the calmodulin-binding site by photoaffinity labeling with ^{125}I -azidocalmodulin. A 230 nm affinity for calmodulin was estimated by displacement of two different concentrations of the ^{125}I -azidocalmodulin with unmodified calmodulin and subsequent Dixon plot analysis. This calmodulin-binding protein is present in erythrocytes at 30,000 copies/cell and is associated exclusively with the membrane. It is tightly bound to a site on red cell cytoskeletons and is totally solubilized in the low ionic strength extract derived from red cell ghost membranes. Visualization of this calmodulin-binding protein in the electron microscope by rotary shadowing, negative staining, and unidirectional shadowing indicates that it is a flattened circular molecule with a 12.4-nm diameter and a 5.4-nm height. Affinity-purified antibodies against the calmodulin-binding protein identify a cross-reacting $M_r = 100,000$ polypeptide(s) in brain membranes.

The erythrocyte membrane has provided a simplified system for study of the function and structure of cell membranes. The result of experiments in the last 15 years has been elucidation of a structural organization of the erythrocyte membrane in which the lipid bilayer is supported on its cytoplasmic surface by an anastomosing network of structural proteins that has often been referred to as the cell's membrane skeleton or "cytoskeleton." The membrane skeleton is linked to the bilayer via a complex between the integral membrane

protein band 3¹ and the membrane linkage protein, ankyrin (for review see Cohen, 1983; Goodman and Schiffer, 1983; Bennett, 1985). This membrane skeleton can be isolated intact as an insoluble residue following extraction of the membrane's lipids and integral proteins with nonionic detergents (Yu *et al.*, 1973) and is composed principally of spectrin, band 4.1,¹ actin, ankyrin, and a number of other less abundant associated polypeptides that have remained uncharacterized. With the discovery of analogues of spectrin (Glenney *et al.*, 1982a, 1982b; Bennett *et al.*, 1982), ankyrin (Davis and Bennett, 1984), and band 4.1 (Cohen *et al.*, 1982; Granger and Lazarides, 1984; Goodman *et al.*, 1984; Baines and Bennett, 1985) in brain and other tissues, the structure of the red cell membrane skeleton has gained increased relevance for the study of the molecular organization of the cytoskeletons of more complex cells.

In spite of the advances described above, knowledge of the structural organization of the red cell membrane remains incomplete. New proteins of the erythrocyte membrane and membrane skeleton have been identified and characterized, such as erythroid forms of myosin and tropomyosin (Fowler and Bennett, 1984; Fowler *et al.*, 1985) and band 4.9,¹ an erythrocyte membrane associated protein that bundles actin (Siegel and Branton, 1985). Other unanswered questions center on the dynamic state of the red cell membrane. Red cells undergo distinct shape changes upon ATP depletion and elevation of intracellular calcium (Weed *et al.*, 1969). Isolated red cell membranes have also been shown to undergo analogous shape changes modulated by ATP and calcium (Sheetz and Singer, 1977; Quist, 1980). These phenomena suggest that the structural organization of the membrane is subject to regulation. Thus, it is of considerable interest that calmodulin, the calcium-activated regulatory protein (for review see Cheung, 1980), binds to uncharacterized membrane-associated proteins in erythrocytes distinct from spectrin or the CaM^{2-} -activated ($\text{Ca}^{2+} + \text{Mg}^{2+}$)-ATPase (Agre *et al.*, 1983).

We describe here the identification and purification, in milligram quantities, of a new membrane-associated protein from red cells that binds calmodulin with a K_d of 230 nM. This ghost calmodulin-binding protein is characterized in terms of its physical properties, interaction with calmodulin, and its molecular dimensions determined by electron microscopy. In addition, immunological evidence is presented for the existence of an analogous protein in brain.

* This research was supported by National Institutes of Health Grants R01 AM19808, R01 GM33996, and Research Career Development Award AM00926 and Grant DAMD 17-83-C-3209 from the Army. The costs of publication of this article were defrayed in part by the payment of page charges. This article must therefore be hereby marked "advertisement" in accordance with 18 U.S.C. Section 1734 solely to indicate this fact.

† To whom correspondence should be addressed: Dept. of Cell Biology and Anatomy, Johns Hopkins University School of Medicine, 725 N. Wolfe St., Baltimore, MD 21205.

¹ After the nomenclature for erythrocyte membrane proteins described by Steck (1974).

² The abbreviations used are: CaM, calmodulin; SDS, sodium dodecyl sulfate; PMSF, phenylmethylsulfonyl fluoride; NaEGTA, ethylene glycol bis(β -aminoethyl ether)-N,N,N',N'-tetraacetic acid sodium salt; HEPES, 4-(2-hydroxyethyl)-1-piperazineethanesulfonic acid; DTT, dithiothreitol.

EXPERIMENTAL PROCEDURES

Materials—Carrier-free Na^{125}I was purchased from Amersham Corp. ^{125}I -Bolton Hunter obtained was from ICN. Plastic thin layer sheets coated with 0.1 mm of cellulose were from Merck. DEAE-53 cellulose was from Whatman. Diisopropylfluorophosphate, leupeptin, Trizma (Tris base), pepstatin A, PMSF, DTT, EGTA, HEPES, Triton X-100, and 1,10-phenanthroline were purchased from Sigma. Polyethylene glycol 8000 was from Fisher. Dextran T-500, Sepharose 4B, cyanogen bromide-activated Sepharose 4B, Protein A, Protein A-Sepharose, Sephacryl S-400, and phenyl-Sepharose CL-4B were from Pharmacia. Leuko-Pak Leukocyte Filters were from Fenwal Laboratories. Nitrocellulose paper and electrophoresis reagents were from Bio-Rad. Sucrose and urea were from Schwarz/Mann. α -Chymotrypsin (54 units/mg) was from Worthington. 400-Mesh copper grids were from Ernest F. Fullam, Inc., and Formvar-coated 200-mesh copper grids were from Ted Pella Inc. *N*-Hydroxysuccinimidyl 4-azidobenzoate was from Pierce. Protein sedimentation and molecular weight standards were from Boehringer Mannheim. Calmodulin was purified from frozen porcine brain by phenyl-Sepharose chromatography, according to Gopalakrishna and Anderson (1982), followed by high performance liquid chromatography on a Pharmacia Mono Q anion exchange column. Frozen porcine brains were obtained from Pel-Freez. Human donor blood (4 units of whole blood) was obtained from a local community blood bank and processed within 48 h of drawing.

Methods—Protein determinations were performed by the procedure of Lowry *et al.* (1951) or Bradford (1976) with bovine serum albumin as a standard. SDS-polyacrylamide electrophoresis was performed with the buffers of Fairbanks *et al.* (1971), on 1.5-mm thick, 3.5–17% exponential gradient slab gels in 0.2% (w/v) SDS. Molecular weights were estimated from curves in which erythrocyte membrane proteins were used as standards (Bennett and Stenbuck, 1980). In experiments that required the fractionation of large (100- μl) sample volumes, SDS-polyacrylamide electrophoresis was carried out in 0.2% (w/v) SDS with the buffers of Laemmli (1970), on 1.5-mm thick 7.5% slab gels and a 2.5-cm 5% stacking gel. Proteins were radioiodinated with Na^{125}I using chloramine-T as an oxidant (Hunter and Greenwood, 1962). Calmodulin was iodinated with Bolton-Hunter reagent (Bolton and Hunter, 1973) as previously described (Agre *et al.*, 1983). Autoradiography was performed at -100°C with either dried polyacrylamide gels or nitrocellulose on X-Omat AR film (Kodak) and Cronex intensifier screens (DuPont).

Membrane Preparation—Erythrocytes were isolated essentially as described by Bennett (1983) from 4 units of donor whole blood by sedimentation at $1 \times g$ in 5 volumes of 150 mM NaCl, 5 mM sodium phosphate, pH 7.5, 0.75% (w/v) Dextran T-500 (Boyam, 1968), and passage over a Leuko-Pak leukocyte filter. This procedure yielded a suspension of erythrocytes virtually free of contamination with any other cell type. The cells were then washed 3 times with 5 volumes of 10 mM sodium phosphate, pH 7.5, 150 mM NaCl at 4°C in 10 volumes (7 liters) of 7.5 mM sodium phosphate, 1 mM NaEGTA, 1 mM DTT, and 0.01% (v/v) diisopropylfluorophosphate. The membranes were harvested and washed in the same buffer according to the procedure of Gietzen and Kolandt (1982) by filtration through a Millipore Pellicon Cassette system equipped with a Durapore filter (0.5- μm pore size). The washed ghost membranes were pre-extracted by the addition of NaCl to a final concentration of 50 mM and collected by sedimentation at $18,000 \times g$ for 40 min at 4°C .

Triton X-100-extracted ghost membranes were prepared essentially by the procedure of Bennett and Stenbuck (1980). The membranes isolated as described above were incubated 15 min at 4°C in 10 volumes of 10 mM sodium phosphate, 100 mM NaCl, 1 mM NaEDTA, 0.5% Triton X-100, 200 $\mu\text{g}/\text{ml}$ PMSF, 4 $\mu\text{g}/\text{ml}$ pepstatin A, 4 $\mu\text{g}/\text{ml}$ leupeptin, pH 7.5, and the extracted membranes were collected by centrifugation at $18,000 \times g$ for 40 min at 4°C . The supernatant was discarded, and the pelleted membranes were resuspended and washed a second time in the same buffer followed by 3 more washes in the same buffer minus Triton X-100.

Antibodies against the ghost calmodulin-binding protein were prepared as described (Davis and Bennett, 1983), except that antibody was eluted with 0.2 M glycine HCl, pH 2.3, instead of with 1 M acetic acid, pH 3.0. Purified calmodulin-binding protein was further fractionated for immunization by SDS-polyacrylamide electrophoresis. Both polypeptides ($M_r = 103,000$ and $97,000$) were excised, and the acrylamide/protein mixture (0.4 mg of protein) was injected into each rabbit as described (Bennett and Davis, 1982). Specific antibodies

against the calmodulin-binding protein were prepared using calmodulin-binding protein cross-linked to Sepharose 4B (0.5 mg/ml) as an immunoadsorbent. Nonimmune antibody was isolated from the pooled serum of naive rabbits according to the same procedure using Protein A-Sepharose 4B (Davis and Bennett, 1983). Immunoblot analysis of proteins transferred electrophoretically from SDS-polyacrylamide gels to nitrocellulose paper was performed as described (Bennett and Davis, 1981).

Preparation of Azidocalmodulin Photoaffinity Label—The photoaffinity label for calmodulin-binding proteins was prepared by a modification of the procedure of Andreassen *et al.* (1981) with the photoaffinity cross-linker *N*-hydroxysuccinimidyl 4-azidobenzoate (Goewert *et al.*, 1982) instead of methyl 4-azidobenzimidate. In short, 10 μl of a 5.0 mg/ml solution of *N*-hydroxysuccinimidyl 4-azidobenzoate dissolved in dimethyl sulfoxide was added to 110 μl of ^{125}I -labeled calmodulin (84,000–114,000 cpm/pmol at a final concentration of 0.35 mg/ml in 10 mM sodium phosphate, 50 μM CaCl_2 , pH 8.1, prepared as indicated above) and incubated 90 min in the dark at 4°C . The solution was then diluted by the addition of 300 μl of 10 mM sodium phosphate, 50 μM CaCl_2 , pH 7.5, and dialyzed overnight against the same buffer in the dark at 4°C . This procedure yields a preparation of ^{125}I -labeled azidocalmodulin at a 5 μM final concentration.

Electron Microscopy—Magnification was calibrated by use of the spacing of 21,600 lines/cm test grids (Ernest Fullam Inc.) and the 39.5-nm spacing (Cohen and Longley, 1966) of vertebrate skeletal muscle tropomyosin paracrystals (a gift from Dr. T. D. Pollard, Department of Cellular Biology and Anatomy, Johns Hopkins School of Medicine). Cross-calibration with each method differed by less than 1%.

Negative staining was performed on Formvar-coated 400-mesh grids with 0.75% uranyl formate according to the procedure of Aeby *et al.* (1981). For shadowed specimens, protein was suspended at approximately 10 $\mu\text{g}/\text{ml}$ in 0.1 M ammonium formate, 30% glycerol (Shotton *et al.*, 1979) sprayed onto freshly cleaved mica sheets, and platinum/carbon shadowed in a Polaron P650A Vacuum Coater evacuated to $1-2 \times 10^{-7}$ torr. Rotary shadowed preparations were shadowed at an angle of 6° and unidirectional shadowing was done at 10° . Molecular dimensions were measured from prints at magnifications of either $\times 313,000$ or $\times 152,000$ with an ocular micrometer graduated at 0.1 mm. Molecular heights were determined from the shadow lengths of unidirectionally shadowed specimens according to the following equation:

$$H = L \times \tan(\alpha)/M.$$

Where H = height in nanometers, L = length of shadow in centimeters, (α) = angle of shadowing (10°), and M = magnification. Measurements were made of unidirectionally shadowed fields in which horse spleen ferritin (height = 12.1 nm, Duong *et al.*, 1985; Fischbach and Andereg, 1965) was included as an internal standard.

Physical Properties—Sedimentation coefficients were estimated by rate-zonal sedimentation on 5–20% sucrose gradients dissolved in 10 mM HEPES, 100 mM NaCl, 0.25 mM NaEGTA, 1.0 mM DTT, pH 7.3, in a SW 50.1 rotor (Martin and Ames, 1961) with standards of human erythrocyte spectrin dimer (8.4 $S_{20,w}$), rabbit muscle aldolase (7.3 $S_{20,w}$), bovine serum albumin (4.6 $S_{20,w}$), and cytochrome *c* (1.75 $S_{20,w}$). The Stokes radius (R_s) was estimated by gel filtration on a Sephacryl S-400 column (0.9 \times 60 cm) equilibrated in 10 mM HEPES, 100 mM NaCl, 0.25 mM NaEGTA, 1.0 mM DTT, pH 7.3, and calibrated with standard proteins of human erythrocyte spectrin dimer ($R_s = 12.3$ nm), *Escherichia coli* β -galactosidase ($R_s = 6.8$ nm), bovine liver catalase ($R_s = 5.2$ nm), and ovalbumin ($R_s = 2.84$ nm). The Stokes radius was estimated from a standard curve of K_{av} versus R_s , as described by Siegel and Monty (1966), with K_{av} determined as defined by Laurent and Killander (1964). Amino acid analysis was performed on a Durrum D-500 instrument by Dr. Joel Shaper, Department of Oncology, Johns Hopkins School of Medicine. Samples of protein (100–120 μg) were hydrolyzed for 24 h at 110°C in constant boiling HCl (Pierce Chemical Co.) with phenol.

RESULTS

Purification and Properties of the Ghost Calmodulin-binding Protein—Following the initial report that identified calmodulin-binding proteins, distinct from spectrin, in the low salt extract of red cell ghosts (Agre *et al.*, 1983), initial attempts to isolate these proteins by calmodulin affinity chromatogra-

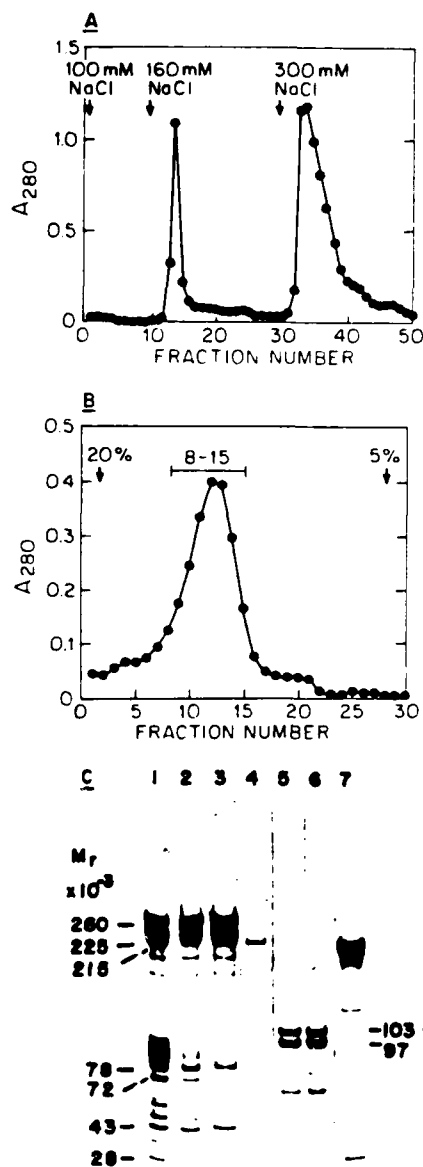


FIG. 1. Purification of human erythrocyte ghost calmodulin-binding $M_r = 103,000$ and $97,000$ polypeptides by DEAE-chromatography and preparative rate-zonal sedimentation on sucrose gradients. The erythrocyte calmodulin-binding $M_r = 103,000$ and $97,000$ polypeptides were solubilized from Triton X-100-extracted ghost membranes (prepared as described under "Experimental Procedures") by resuspension in 1 ghost volume (680 ml) of 1.0 M NaCl, 1 mM NaEDTA, 10 mM sodium phosphate, 1 mM DTT, 200 μ g/ml PMSF, 4 μ g/ml pepstatin, and 4 μ g/ml leupeptin, pH 7.5. After a 30-min incubation at 4 $^{\circ}$ C, the suspension was centrifuged for 45 min at 40,000 rpm in a 45 Ti rotor at 4 $^{\circ}$ C. The supernatant was collected and dialyzed overnight against 20 liters of 10 mM sodium phosphate, 50 mM NaCl, 0.25 mM NaEGTA, and 1 mM DTT, pH 7.5. After dialysis, the supernatant was loaded onto a 12-ml DE53-cellulose column that had been equilibrated in the same buffer. The column was washed with 30 ml of the equilibration buffer at 100 mM NaCl and then eluted with 60 ml of the same buffer at 160 mM NaCl followed by a final elution with 60 ml of the buffer at 300 mM NaCl. 3.0-ml fractions were collected (see panel A). Fractions 13-16 from the 160 mM NaCl elution were pooled and concentrated to 3.5 ml against polyethylene glycol 8000 flakes and layered onto a 30-ml linear 5-20% sucrose gradient dissolved in 10 mM HEPES, 100 mM NaCl, 0.25 mM NaEGTA, and 1 mM DTT, pH 7.5. The gradient was

TABLE I

Summary of purification of erythrocyte membrane-associated calmodulin-binding $M_r = 103,000$ and $97,000$ polypeptides

Fraction	Protein mg	% Protein as calmodulin- binding pro- tein ^a	Purifi- cation -fold	Yield %
Ghosts	2442	1.0		
Triton X-100-extracted ghosts	1,438	2.6	2.6	100
1 M NaCl pellet	950	2.4		57
1 M NaCl supernatant	138	7.9	7.9	27
DEAE-52 150 mM NaCl elution	5.9	83.0	83.0	12
5-20% sucrose gradient peak	3.3	96.5	96.5	8

^a Calculated from densitometer scans of SDS gels stained with Coomassie Blue (Fig. 1) and based on the total amount of protein present as bands with $M_r = 103,000$, $97,000$, $74,000$, $62,000$, and $54,000$.

phy revealed two major calmodulin-binding polypeptides of $M_r = 103,000$ (α) and $97,000$ (β). These peptides are also present in a 0.5 M NaCl extract of ghost membranes (data not shown) as well as the 1.0 M NaCl extract of the Triton X-100-insoluble residue of ghost membranes or cytoskeleton. Of the three extracts, the high salt extract of the cytoskeletons showed the least amount of degradation; therefore, this extract was used as the starting material for the purification of the $M_r = 103,000$ and $97,000$ calmodulin-binding polypeptides. The 1 M NaCl extract of cytoskeletons, in which ankyrin accounts for 80% of the protein (Bennett and Stenbuck, 1980), is 8-fold enriched over ghost membranes in the $M_r = 103,000$ and $97,000$ polypeptides (see Table I). The $M_r = 103,000$ and $97,000$ polypeptides were purified by DE53-cellulose chromatography and preparative rate-zonal sucrose gradient sedimentation (Fig. 1). The 160 mM elution step of the DE53 chromatography yields a highly enriched preparation that contains the $M_r = 103,000$ and $97,000$ polypeptides at greater than 70% of the total protein and, in addition, some minor polypeptides of $M_r = 74,000$, $62,000$, $54,000$, $48,000$, and $43,000$. Preparative rate-zonal sucrose gradient sedimentation yields 3-5 mg of a highly homogeneous preparation of the $M_r = 103,000$ (α) and $97,000$ (β) subunits in a 0.8 (α/β)² stoichiometry with trace amounts of the $M_r = 74,000$, $62,000$, and $54,000$ polypeptides (see Fig. 1, panel C). The purification can be completed within 60 h of the initial lysis of the red cells with a final yield of 8% (Table I).

The $M_r = 103,000$ and $97,000$ subunits are distinct polypep-

² This stoichiometry (0.8) is lower than the expected ratio of 1.0 due to disproportionate degradation of CaM-BP_{103/97}. This value decreases in more degraded preparations of CaM-BP_{103/97}, thus indicating that the α subunit is more susceptible to proteolysis.

centrifuged 10.5 h at 38,000 rpm in a Beckman VTi 50 rotor at 4 $^{\circ}$ C and 1.25-ml fractions were collected from the bottom of the tube (see panel B). Samples from each step in the purification procedure were analyzed by SDS electrophoresis (see "Experimental Procedures") and stained with Coomassie Blue: ghost membranes, 25 μ g of protein (lane 1); Triton X-100-extracted ghosts, 15 μ g of protein (lane 2); Triton X-100-extracted ghosts after 1 M NaCl extraction, 15 μ g of protein (lane 3); protein solubilized from Triton-extracted ghosts and loaded onto DE52 column, 2 μ g of protein (lane 4); 160 mM NaCl elution from the DE52 chromatography, 5 μ g of protein (lane 5); pooled fractions 8-15 from the sucrose gradient, 8 μ g of protein (lane 6); 300 mM NaCl elution from the DE52 chromatography, 12 μ g of protein (lane 7). The asterisk indicates proteolytically derived polypeptides (see Fig. 2) of $M_r = 74,000$, $62,000$, and $54,000$.

tides that are not proteolytically derived from one another. This is demonstrated by their distinct chymotryptic fingerprints (see Fig. 2). The three minor polypeptides are proteolytic fragments of the $M_r = 103,000$ (α) and $97,000$ (β) subunits. As is shown by the fingerprints of these three minor polypeptides, the $M_r = 74,000$ polypeptide is derived from the $M_r = 103,000$ α subunit, whereas the $M_r = 62,000$ and $54,000$ polypeptides are derived from the $M_r = 97,000$ β subunit.

All three of the proteolytic fragments of $M_r = 74,000$, $62,000$, and $54,000$ appear to migrate intact with the parent molecule via noncovalent associations since they continued to copurify with the $M_r = 103,000$ and $97,000$ subunits at equal stoichiometries under several dissociating conditions (results not shown) which include: 1) gel filtration in 1 M NaCl; 2) hydroxylapatite chromatography in 1 M NaBr; 3) sucrose gradient sedimentation in 0.5 M or 1 M NaBr; and 4) native *versus* SDS-denatured two-dimensional polyacrylamide electrophoresis.

Although the $M_r = 103,000$ and $97,000$ subunits have clearly different peptide maps, a composite map of a mixture of the two polypeptides (see Fig. 2, panel C) indicates that 30% of the major spots are common to both subunits (7 out of 21 peptides). The total number of spots held in common and the fact that they represent major peptides in each map rules out the possibility that the overlap of the two maps is due to the contamination of the $M_r = 97,000$ band with degradation products of the $M_r = 103,000$ and suggests that the α and β subunits share a sequence homology of at least 30%. For convenience, this protein hence will be referred to as CaM-BP_{103/97} in recognition of its subunit composition (see Fig. 1) and ability to bind calmodulin (see Figs. 6–8).

CaM-BP_{103/97} is highly sensitive to proteolysis which may be due to exogenous proteases contributed by the lysosomal enzymes of nonerythrocyte cells or the endogenous protease activity of the erythrocyte, such as the Ca^{2+} -activated calpains of the cytosol (Murakami *et al.*, 1981) or the membrane-

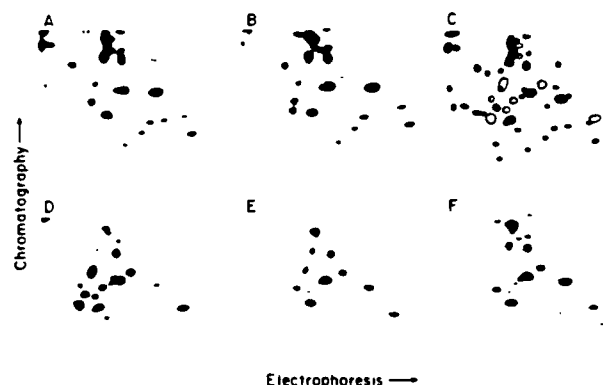


FIG. 2. Two-dimensional peptide map analysis of the $M_r = 103,000$, $97,000$, $74,000$, $62,000$, and $54,000$ polypeptides of the ghost calmodulin-binding protein. The ghost calmodulin-binding polypeptides, purified as described in Fig. 1, were ^{125}I -labeled with 1 mCi of Na^{125}I by oxidation with chloramine-T (see "Experimental Procedures"). The labeled protein was fractionated by SDS-polyacrylamide electrophoresis, stained with Coomassie Blue, and the polypeptides of $M_r = 103,000$, $97,000$, $74,000$, $62,000$, and $54,000$ (see Fig. 1, lane 6) were excised. The slices were digested with α -chymotrypsin and peptide maps were prepared as described (Davis and Bennett, 1982): $M_r = 103,000$ β subunit (panel A); $M_r = 74,000$ polypeptide (panel B); $M_r = 97,000$ α subunit (panel D); $M_r = 62,000$ polypeptide (panel E); $M_r = 54,000$ polypeptide (panel F); a composite representation of a mixture of the α and β subunits, darkened spots represent the peptides derived from the α subunit, blank spots represent the peptides derived from the β subunit, and the stippled spots represent peptides common to both the α and β subunits (panel C).

associated acid proteinases (Yamamoto and Marchesi, 1984). Preparations of CaM-BP_{103/97} purified in the absence of protease inhibitors or in steps that involve the addition of calcium are heavily degraded to the proteolytic fragments described above. For this reason, removal of the nonerythrocyte cells by dextran sedimentation and Leuko-Pak filtration and the inclusion of protease inhibitors such as diisopropylfluorophosphatase, PMSF, leupeptin, and pepstatin are essential procedures in the purification of the protein. CaM-BP_{103/97}, purified as described in Fig. 1, can be stored on ice for up to 3 weeks with little degradation and, if stored at -20°C , will remain intact for up to 2 months.

CaM-BP_{103/97} can be cross-linked to a complex of $M_r = 200,000$ by spontaneous or copper 1,10-phenanthroline-induced oxidation. Fig. 3 demonstrates that a major $M_r = 200,000$ complex as well as some minor higher molecular weight complexes can be generated by increasing concentration of copper-saturated 1,10-phenanthroline. These complexes are visible by both Coomassie staining and immunoblot analysis (see Fig. 3). This result indicates that CaM-BP_{103/97} exists in solution mainly as a dimer, although the production of higher molecular weight complexes suggests the possibility of higher order oligomer formation. Because of its sensitivity to oxidation, it was necessary to include reducing agent during all stages of the purification and storage of CaM-BP_{103/97} and to completely remove Triton X-100 (which contains contaminating peroxides) from the cytoskeletons (see "Experimental Procedures").

CaM-BP_{103/97} is a dimer in solution as indicated by its calculated M_r of 197,000 determined from a Stokes radius (R_s)

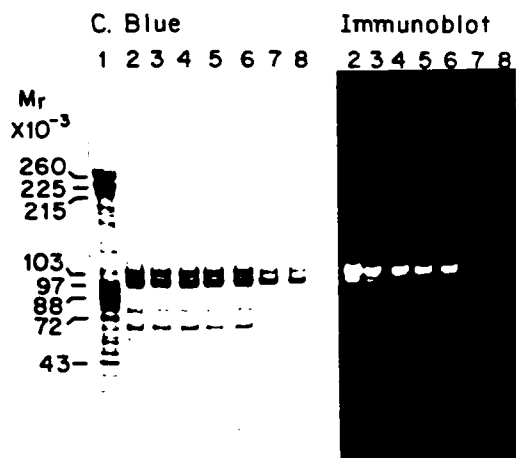


FIG. 3. Copper/phenanthroline-induced oxidative cross-linking of purified CaM-BP_{103/97}. Samples in lanes 3–8 contain purified CaM-BP_{103/97} that had been incubated at $200\text{ }\mu\text{g/ml}$ in a $50\text{-}\mu\text{l}$ volume of 5 mM HEPES, 50 mM NaCl, 0.5 mM CuCl_2 , pH 7.3, for 1 h at 24°C with 0, 10, 20, 50, 80, or $100\text{ }\mu\text{M}$ 1,10-phenanthroline. The oxidation was quenched by the addition of $10\text{ }\mu\text{l}$ of 10 mg/ml *N*-ethylmaleimide, $10\text{ }\mu\text{l}$ of 10 mM NaEDTA, and $17\text{ }\mu\text{l}$ of 5-fold concentrated SDS-polyacrylamide gel electrophoresis buffer as described (Wang and Richards, 1974). The samples were then incubated at 37°C for 30 min and fractionated by SDS-polyacrylamide electrophoresis. Parallel lanes were transferred to nitrocellulose and prepared for immunoblot analysis with affinity-purified IgG (see Fig. 4) as described (see "Experimental Procedures"): ghost membrane (lane 1); CaM-BP_{103/97} fully reduced by heating to 50°C with 0.1 M DTT in SDS-polyacrylamide gel electrophoresis buffer prior to quenching (lane 2); CaM-BP_{103/97} oxidized as described above with 1,10-phenanthroline at concentrations of $0\text{ }\mu\text{M}$ (lane 3); $10\text{ }\mu\text{M}$ (lane 4); $20\text{ }\mu\text{M}$ (lane 5); $50\text{ }\mu\text{M}$ (lane 6); $80\text{ }\mu\text{M}$ (lane 7); and $100\text{ }\mu\text{M}$ (lane 8). Asterisk indicates the $M_r = 200,000$ band formed by the oxidative cross-linking of the CaM-BP_{103/97} $M_r = 103,000$ and $97,000$ polypeptides.

of 6.8 nm, a sedimentation coefficient of 6.8 $S_{20,w}$, and a calculated partial specific volume of 0.73 cm^3/g (see Table II). CaM-BP_{103/97} is most likely a heterodimer rather than a mixture of homodimers of the $M_r = 103,000$ and the $M_r = 97,000$ subunit since (a) both polypeptides are isolated in a constant stoichiometric ratio by CaM-Sepharose affinity chromatography (see Fig. 6) and the various fractionation procedures, described above; (b) ^{125}I -azidocalmodulin affinity labeling only modifies the $M_r = 97,000$ subunit of CaM-BP_{103/97} (see below, Fig. 7) even though both the $M_r = 103,000$ and the $M_r = 97,000$ subunits are quantitatively retained on CaM-Sepharose, suggesting that the $M_r = 103,000$ (α) subunit is retained due to a tight noncovalent linkage to the $M_r = 97,000$ (β) subunit.

Affinity-purified Ig directed against CaM-BP_{103/97} was prepared from the immune serum of rabbits that were inoculated with a 1:1 mixture of electrophoretically purified $M_r = 103,000$ and 97,000 CaM-BP_{103/97} polypeptides (see "Experimental Procedures"). The characterization of the purified antibody, by immunoblot analysis (Fig. 4), shows that, in ghosts, the antibody cross-reacts exclusively with the CaM-BP_{103/97} polypeptides. This result demonstrates that the CaM-BP_{103/97} polypeptides are not degradation products of larger molecular weight membrane proteins. In addition, the degradation products of $M_r = 74,000$, 52,000, and 64,000 cross-react. The asterisk (lane 3 of the right panel of Fig. 3) indicates the cross-reacting band of $M_r = 200,000$ formed by spontaneous oxidation of CaM-BP_{103/97} (see Fig. 3).

The amount of CaM-BP_{103/97} in intact red cells and ghost membranes was estimated by a quantitative immunoblot procedure using a standard curve of purified CaM-BP_{103/97}. CaM-BP_{103/97} is present per cell at 30,000 copies with greater than 95% associated exclusively with the membrane (see Table III).

TABLE II
Summary of physical properties of CaM-BP_{103/97}

Property	Value
Stokes radius ^a	6.9 nm
Sedimentation coefficient, $S_{20,w}$ ^b	6.8 S
Partial specific volume, \bar{v} ^c	0.73
M_r , calculated ^d	197,000
Extinction coefficient, $E_{279\text{nm}}^{1\%}$ ^e	6.24
Frictional ratio, f/f_0 ^d	1.56
M_r , SDS electrophoresis ^f	103,000 (α) 97,000 (β)
Subunit stoichiometry, (α/β) ^f	0.8

^a Estimated from gel filtration (see "Experimental Procedures").

^b Estimated from sedimentation on 5–20% sucrose gradients (see "Experimental Procedures").

^c Calculated from the amino acid composition as described (Cohn and Edsall, 1943).

^d Calculated according to the following equations (Tanford, 1961):

$$M_r = \frac{6\pi N R_s S_{20,w}}{1 - \bar{v}\rho_{20,w}}$$

and

$$f/f_0 = R_s \left(\frac{4\pi N}{3M_r (\bar{v} + \delta\rho)} \right)^{1/3}$$

with an assumed hydration δ of 0.4 g of solvent/g of protein (Kuntz and Kauzmann, 1974).

^e Derived from standard protein curves determined by the methods of Lowry *et al.* (1951) and Bradford (1976).

^f Estimated from mobility on SDS gels calibrated as described (Bennett and Stenbuck, 1980).

^g Determined by densitometer scans of SDS gels stained with Coomassie Blue (Fig. 1). The value reflects the ratio between the intact polypeptides of $M_r = 103,000$ and 97,000.

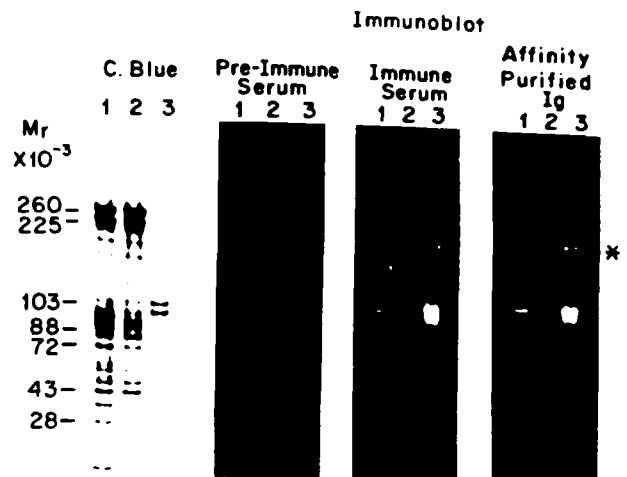


FIG. 4. Isolation of IgG against CaM-BP_{103/97} by immunoadsorption with antigen immobilized on Sepharose 4B. Ghost membranes (lane 1), Triton X-100-extracted ghost membranes (lane 2), and purified CaM-BP_{103/97} (lane 3) were electrophoresed on SDS-polyacrylamide gels and stained with Coomassie Blue (C. Blue) (outer left panel). Three sets of parallel lanes were transferred electrophoretically to nitrocellulose (see "Experimental Procedures") and incubated with either a 1:100 dilution of preimmune serum, a 1:100 dilution of immune serum, or affinity-purified anti-CaM-BP_{103/97} antibody (0.14 $\mu\text{g}/\text{ml}$ protein) prepared as described (see "Experimental Procedures"). The asterisk indicates a $M_r = 200,000$ band that represents a CaM-BP_{103/97} heterodimer formed by oxidative cross-linking of internal sulphhydryl groups (see Fig. 3).

TABLE III
Quantitation of the amount of CaM-BP_{103/97} in the erythrocyte

Sample	Copies/cell ^a
Intact red cells ^b	30,000
Cytosol ^b	<1,500
Ghost membranes ^c	33,000

^a Determined by a quantitative immunoblot from a linear standard curve of known concentrations of purified CaM-BP_{103/97}. Duplicate samples were reproducible within 5%.

^b The number of intact cells/sample was quantitated by measurement in a hemacytometer. Samples of pact cells were diluted 1:15. Cytosol sample was prepared by pelleting the membranes from the hemolysate of a 1:15 dilution of the pact cells. Equal volumes of pact cells and cytosol were assayed.

^c Cell equivalents of ghost membranes were determined by standardizing the amount of spectrin in the ghost membranes to that of intact cells by densitometric scanning of Coomassie Blue-stained gels.

Selective Solubilization of CaM-BP_{103/97} from the Erythrocyte Membrane—Immunoblot analysis of whole cells and membrane-depleted cytosol shows that CaM-BP_{103/97} is completely membrane-bound with no detectable amounts in the cytosol (Fig. 5). Extraction of spectrin and actin with low salt completely solubilized CaM-BP_{103/97} from the membrane. Less than 10% of the CaM-BP_{103/97} is solubilized during the initial Triton X-100 extraction of ghost membranes, and subsequent extractions with Triton X-100 fail to elute any additional cross-reactivity (see Fig. 5, lanes 6–9). Extraction with 1 M NaCl released only 30% of the CaM-BP_{103/97} from the membrane skeletons, while the remainder of CaM-BP_{103/97} remains tightly bound and can only be removed by conditions that dissolve the entire cytoskeletal assembly (see Fig. 5, lanes 10 and 11). Thus, the major population of CaM-BP_{103/97} is tightly linked to site(s) on the membrane skeleton.

Ca²⁺-dependent Binding of CaM-BP_{103/97} to Calmodulin—Calcium-dependent binding of CaM-BP_{103/97} to calmodulin is demonstrated by calmodulin-Sepharose 4B affinity chroma-

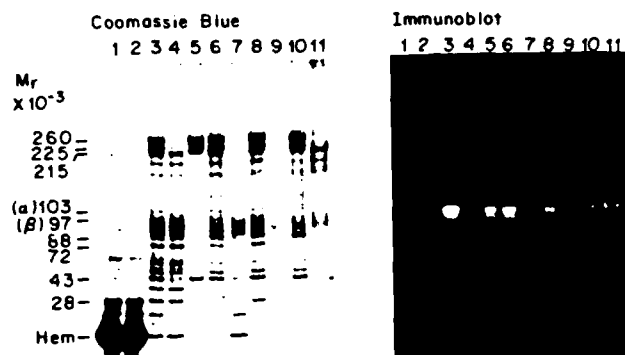


FIG. 5. Selective solubilization of CaM-BP_{103/97} from erythrocyte ghost membranes. Samples were fractionated by electrophoresis on SDS polyacrylamide gradients and stained with Coomassie Blue. Parallel lanes were transferred electrophoretically to nitrocellulose and prepared for immunoblot analysis (see "Experimental Procedures"): total red cell lysate (lane 1); 100,000 \times *g* membrane-depleted lysate "cytosolic fraction" (lane 2); ghost membranes (lane 3); spectrin-depleted inside-out vesicles prepared by low salt extraction of ghost membranes prepared as described (Bennett, 1983) (lane 4); spectrin-containing supernatant from the low salt extraction (lane 5); Triton X-100-extracted ghost membranes (pellet from the first extraction, see "Experimental Procedures") (lane 6); supernatant from Triton X-100 extraction of ghost membranes (lane 7); pellet from second Triton X-100 extraction of ghost membranes (lane 8); supernatant from the second Triton X-100 extraction of ghost membranes (lane 9); pellet from the 1 M NaCl extraction of the Triton X-100-treated ghost membranes (see "Experimental Procedures") (lane 10); 2 \times concentrated supernatant from the 1 M NaCl extraction of the Triton X-100-treated ghost membranes (lane 11).

tography and photoaffinity labeling with ¹²⁵I-azidocalmodulin. The CaM-BP_{103/97} in the 1 M NaCl extract of the cytoskeletons is quantitatively retained on a calmodulin-Sepharose 4B affinity column in the presence of 10 μ M CaCl₂. Ankyrin, the major protein in the extract loaded on the affinity column, was not adsorbed in the presence of calcium (Fig. 6, lanes 2 and 3). When the column is washed with 5 mM NaEGTA, the protein eluted is highly enriched in CaM-BP_{103/97}. The CaM affinity step results in a 10-fold enrichment in CaM-BP_{103/97} over the starting material, based on densitometry of Coomassie Blue-stained gels. In addition to CaM-BP_{103/97}, there are two minor bands of $M_r = 48,000$ and $43,000$ and several other very faint high molecular weight bands present in the eluted protein. These polypeptides could be binding to the column by either direct association with calmodulin or via a complex with CaM-BP_{103/97}. The CaM-BP_{103/97} in the eluted material is proteolysed due to the exposure of the crude extract to calcium (see Fig. 2), as indicated by the increased amount of CaM-BP_{103/97} present as the $M_r = 74,000$, $62,000$, and $54,000$ degradation products (Fig. 6, lane 4).

Photoaffinity labeling of CaM-BP_{103/97} with ¹²⁵I-azidocalmodulin results in the calcium-dependent formation of a $M_r = 113,000$ radioactive band (Fig. 7, lane 2). The $M_r = 97,000$ subunit is the polypeptide labeled with calmodulin, since the formation of a $M_r = 113,000$ β -CaM complex is accompanied by depletion of the $M_r = 97,000$ polypeptide (Fig. 7, right panel). Moreover, the apparent M_r of the complex corresponds to the sum of the molecular weights of calmodulin ($M_r = 16,000$) and the β subunit ($M_r = 97,000$). In addition to the $M_r = 113,000$ complex, a minor radiolabeled complex of $M_r = 70,000$ is detectable only in the presence of calcium. This complex is the result of affinity labeling of the $M_r = 54,000$ polypeptide derived from the β subunit.

Quantitative Displacement of the ¹²⁵I-Azidocalmodulin Photoaffinity Label with Unlabeled Calmodulin—The ¹²⁵I-azido-

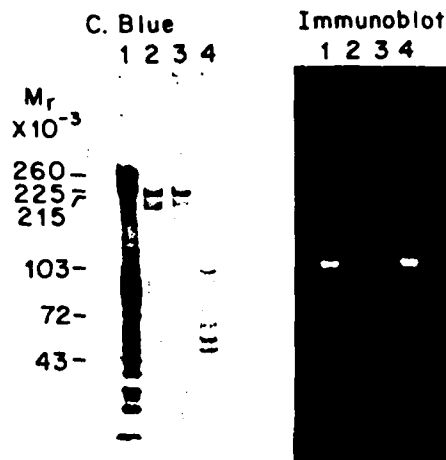


FIG. 6. Isolation of the CaM-BP_{103/97} by affinity chromatography on calmodulin-Sepharose 4B. 20 ml of the 1 M NaCl extract from the Triton X-100-treated ghost membranes (see Fig. 1) was dialyzed overnight against 10 mM HEPES, 100 mM NaCl, 0.25 mM NaEGTA, 1 mM DTT, pH 7.3 and, following dialysis, CaCl₂ (0.25 mM) was added to yield a final free calcium concentration of 10 μ M. The extract was then loaded at 3 ml/h onto a 3-ml calmodulin-Sepharose 4B column (1 mg of calmodulin/ml of Sepharose), washed with 50 volumes of the loading buffer, and eluted with the same buffer plus 5 mM NaEGTA. Samples from each step were prepared for electrophoresis and stained with Coomassie Blue. Parallel lanes were transferred electrophoretically onto nitrocellulose and prepared for immunoblot analysis with affinity-purified anti-CaM-BP_{103/97} IgG (see "Experimental Procedures"): ghost membranes (lane 1); 1 M NaCl extract of Triton X-100-treated ghosts prior to loading onto the CaM-Sepharose (lane 2); protein that broke through the CaM-Sepharose in the presence of calcium (lane 3); protein eluted from the CaM-Sepharose with 5 mM NaEGTA (lane 4).

calmodulin photoaffinity label was displaced from purified CaM-BP_{103/97} with increasing concentrations of unmodified calmodulin in the presence of calcium. Panel A of Fig. 8 is an autoradiograph of the assay in which 100 nM ¹²⁵I-labeled azido-CaM was displaced. Panel B shows the competition curves generated by the displacement of ¹²⁵I-azidocalmodulin at 100 and 500 nM concentrations. At each photoaffinity label concentration, unlabeled calmodulin displaces 50% of the label with less than 500 nM calmodulin. A Dixon plot (Dixon, 1953) of the data (inset of panel B) yields an estimated K_d of 230 nM. This calculated K_d for the native calmodulin indicates that CaM-BP_{103/97} binds calmodulin in the presence of calcium with a K_d of 230 nM.

Electron Microscopic Visualization of CaM-BP_{103/97}—Visualization of CaM-BP_{103/97} in the electron microscope by rotary shadowing with platinum shows that it is a circular molecule (Fig. 9). CaM-BP_{103/97} has a minimum molecular diameter of 12.4 nm based on negatively stained images. A molecular height of 5.4 nm was estimated by measuring shadow lengths of unidirectionally shadowed specimens using ferritin as a standard. CaM-BP_{103/97} thus is a flattened, disc-shaped molecule with a rather high axial ratio of 2.3. This level of asymmetry is consistent with the frictional ratio of 1.56 calculated for the protein from its hydrodynamic properties (see Table II). Ferritin, in contrast, is a spherical protein with a molecular diameter (12.1 nm) that is very close to that of CaM-BP_{103/97}. However, because ferritin is a spherical molecule with an axial ratio that is close to 1 and a molecular weight that is twice that calculated for CaM-BP_{103/97} (Linder et al., 1981), ferritin would be expected to have a much greater height. This is clearly demonstrated in the unidirectionally shadowed samples of the last two panels of column C in Fig.

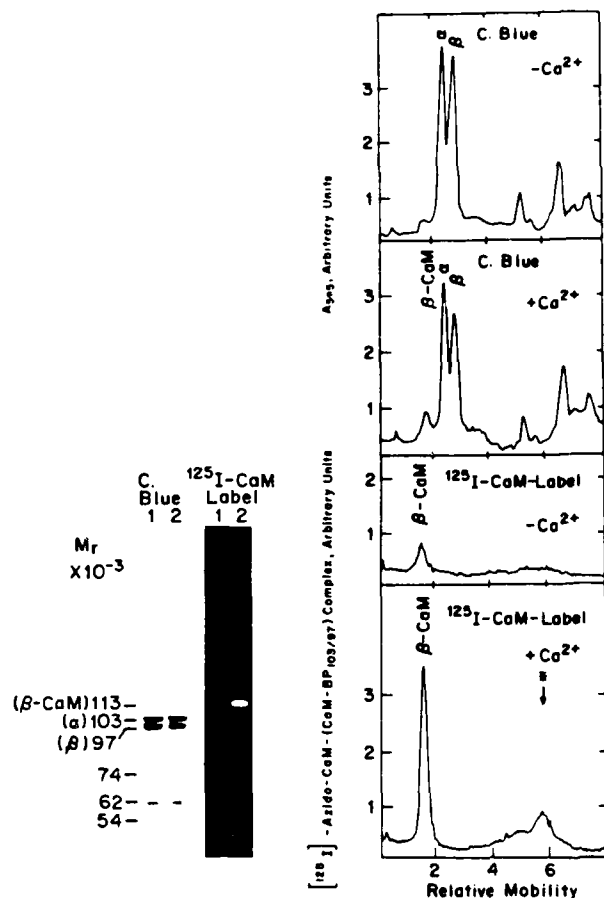


FIG. 7. ^{125}I -Azidocalmodulin photoaffinity labeling of the β subunit of $\text{CaM-BP}_{103/97}$. $42 \mu\text{g/ml}$ $\text{CaM-BP}_{103/97}$ was incubated 1 h in the dark at 4°C in a $100\text{-}\mu\text{l}$ volume of 10 mM HEPES, $\text{pH } 7.3$, 100 mM NaCl, 1 mM DTT, and 2.5 mM NaEGTA with $0.8 \mu\text{M}$ ^{125}I -azidocalmodulin in the absence or presence of 2.5 mM CaCl_2 . At the end of the incubation, the samples were UV-irradiated at 2 cm with a model R52G UV lamp (Ultraviolet Products Inc.). The $100\text{-}\mu\text{l}$ samples were then prepared for electrophoresis on a 7.5% SDS-polyacrylamide slab gel with 2.5-cm 5% stacker using the buffer system of Laemmli (1970) (see "Experimental Procedures"). The gel was stained with Coomassie Blue, dried down, and an autoradiograph was prepared (see "Experimental Procedures"). The left panel shows the Coomassie Blue-stained gel and the autoradiograph: $\text{CaM-BP}_{103/97}$ with ^{125}I -azidocalmodulin in the absence of calcium (lane 1); $\text{CaM-BP}_{103/97}$ with ^{125}I -azidocalmodulin in the presence of calcium (lane 2). $\beta\text{-CaM}$ denotes the $M_r = 113,000$ complex formed by the $M_r = 97,000$ β subunit of $\text{CaM-BP}_{103/97}$ cross-linked by the photoaffinity label to ^{125}I -azidocalmodulin. The right panel shows a densitometer tracing of the Coomassie Blue-stained gel and autoradiograph. The asterisk indicates the formation of a $M_r = 70,000$ complex between ^{125}I -azidocalmodulin and the $M_r = 54,000$ proteolytic fragment derived from the β subunit (see Fig. 2) visualized by autoradiography.

9, where an example of ferritin alone and a mixture of $\text{CaM-BP}_{103/97}$ with ferritin are shown. As would be expected for a particle that is more than twice the height (12.1 nm) of $\text{CaM-BP}_{103/97}$, ferritin casts a shadow that is twice as long and takes up far more platinum than $\text{CaM-BP}_{103/97}$.

The molecular dimensions determined for $\text{CaM-BP}_{103/97}$ indicate that it has a shape similar to that of a rigid ellipsoid of revolution (Scheraga, 1961). The particular ellipsoid that is closest in shape to $\text{CaM-BP}_{103/97}$ is the oblate ellipse, which is formed by the resolution of an ellipse about its short axis. Several equations have been developed to predict the hydrodynamic behavior of rigid ellipsoids of revolution based on

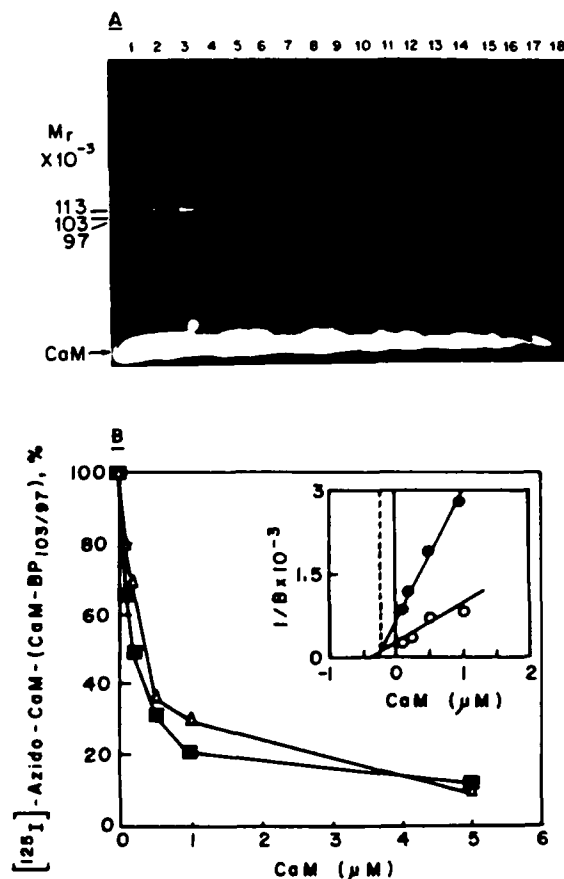


FIG. 8. Displacement of the ^{125}I -azido- CaM photoaffinity label from the $\text{CaM-BP}_{103/97}$ by unlabeled calmodulin. $\text{CaM-BP}_{103/97}$ ($12 \mu\text{g/ml}$) in 10 mM HEPES, 100 mM NaCl, 2.5 mM NaEGTA, $\text{pH } 7.3$, was incubated with either 100 or 500 nM ^{125}I -azidocalmodulin in the presence or absence of 2.5 mM CaCl_2 and displaced by the addition of increasing concentrations of unlabeled CaM . The samples were incubated in the dark for 1 h at 4°C and photolyzed by UV irradiation, and the ^{125}I photoaffinity-labeled complexes were isolated by SDS-polyacrylamide gel electrophoresis as described in Fig. 7. The Coomassie-stained gel was dried down, and the radiolabeled bands were visualized by autoradiography. The regions on the gel corresponding to a migration at $M_r = 113,000$ were excised and assayed for ^{125}I in a γ counter. To ensure that all the samples in the assay received equal irradiation with the UV lamp, the incubation and UV irradiation was done in a 96-well microtiter plate (Nunc). Each point was assayed in duplicate with a standard error of $<4\%$, and the labeling in the absence of calcium was subtracted as background. Panel A is an autoradiograph of the assay in which 100 nM ^{125}I -azidocalmodulin was competed in the presence of calcium with unlabeled calmodulin at concentrations of 0 nM (lanes 2-3); 100 nM (lanes 5-6); 200 nM (lanes 8-9); 500 nM (lanes 11-12); $1 \mu\text{M}$ (lanes 14-15); and $5 \mu\text{M}$ (lanes 17-18). Lanes 1, 4, 7, 10, 13, and 16 were the controls done in the absence of calcium. Panel B shows the displacement curves generated from assay at 100 nM (■) and 500 nM (△) ^{125}I -azidocalmodulin. The inset is a Dixon plot of the assay where the dotted line indicates the point where the intersection of the inhibition curves lies over the x-axis. B = amount of undisplaced label in counts/min.

their axial ratios (Scheraga, 1961; Cantor and Schimmel, 1980) and yield a calculated frictional ratio (f/f_0) of 1.23 for $\text{CaM-BP}_{103/97}$ (see Table IV). This value differs from that predicted from the hydrodynamic properties (1.56) by 21% . The possible significance of this difference will be addressed below. The calculated volume occupied by an oblate ellipse with the dimensions of $\text{CaM-BP}_{103/97}$ can be used along with the partial specific volume and an assumed hydration to

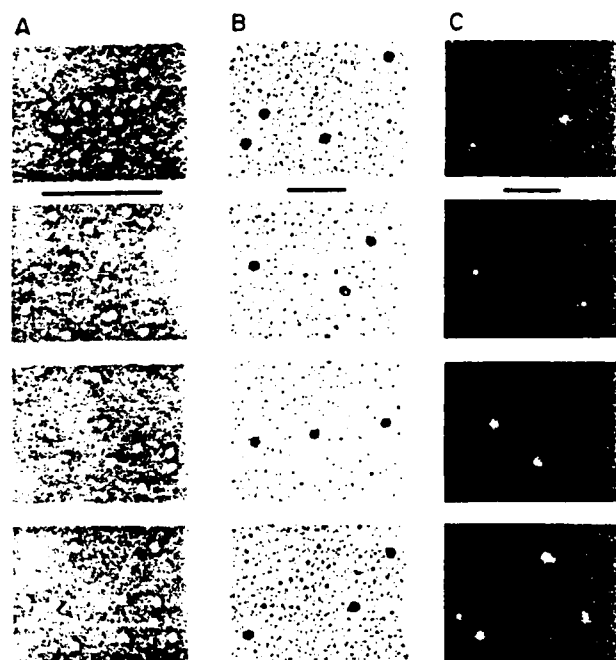


FIG. 9. Electron microscopic visualization of CaM-BP_{103/97} by negative staining, rotary shadowing, and unidirectional shadowing. CaM-BP_{103/97} (approximately 10 μ g/ml) was examined by negative staining (column A); rotary shadowing (column B); and unidirectional shadowing (column C) as described (see "Experimental Procedures"). The 3rd plate from the top in column C shows the ferritin (approximately 20 μ g/ml) alone used as an internal standard for molecular height. The fourth plate in column C is a typical field of the mixtures of ferritin and CaM-BP_{103/97} used to determine the molecular height of CaM-BP_{103/97} from the shadow lengths. The bar = 100 nm.

TABLE IV

Summary of molecular properties of CaM-BP_{103/97} determined by electron microscopy

Property	Value
Molecular diameter	12.4 \pm 1.1 nm ^a
Molecular height	5.4 \pm 0.5 nm ^b
Axial ratio (p)	2.3
M_r , calculated ^c	203,000
Frictional ratio, f/f_0 ^d	1.23

^a The error represents the standard deviation determined from $N = 104$ measurements of negatively stained fields of CaM-BP_{103/97}. This yields a calculated standard error of ± 0.1 nm.

^b The error represents the standard deviation from $N = 75$ measurements of unidirectionally shadowed specimens (see "Experimental Procedures"). This yields a calculated standard error of ± 0.6 nm.

^c This value is determined from the total amount of protein that could occupy the volume of an oblate ellipse with a 12.4 nm diameter and a 5.4-nm height. The calculation assumes a hydration of 0.4 g/g solvent and a partial specific volume of 0.73 cm³/g translates to 0.78 daltons/A³.

^d Derived from the axial ratio (p), by determination of the Perrin factor (F) (Scheraga, 1961; Cantor and Schimmel, 1980), and used in the following equation as described (Duong *et al.*, 1985):

$$f/f_0 = 1/F[(\bar{r} + \delta)/\bar{r}]^{1/3}$$

where

$$F = p^{2/3} \tan^{-1}[(p^2 - 1)^{1/2}]/(p^2 - 1)^{1/2}$$

where $\bar{r} = 0.73$ as determined from the amino acid composition (see Table II) and hydration δ is assumed to be 0.4 g of solvent/g of protein (Kuntz and Kauzmann, 1974).

predict the molecular weight of CaM-BP_{103/97}. By using the same values for hydration and the partial specific volume that were used in the determination of f/f_0 from the hydrodynamic measurements (see Table II), a M_r of 203,000 can be calculated for CaM-BP_{103/97} (see Table IV). This value is in excellent agreement with the values of $M_r = 200,000$ and 197,000 predicted from SDS-polyacrylamide electrophoresis and the hydrodynamic properties, respectively.

Identification of a Polypeptide(s) in Brain that Cross-reacts with Affinity-purified Anti-CaM-BP_{103/97} IgG—The crude membrane fraction of bovine cerebrum was analyzed using antibody against CaM-BP_{103/97} and a polypeptide(s) that migrated slightly faster than the $M_r = 103,000$ α subunit of CaM-BP_{103/97} with an approximate $M_r = 100,000$ was identified (Fig. 10). This cross-reactivity was undetectable in the vesicle fractions (Fig. 10, lane 3), but occurred at a significant level in the cytosolic fraction. This cross-reactive band is a CaM-binding protein since it can be selectively adsorbed out of a crude extract of bovine brain membranes by CaM-Sepharose chromatography. Moreover, affinity labeling of the extract with ¹²⁵I-azidocalmodulin produces a $M_r = 116,000$ radiolabeled band (results not shown). The trivial explanation that this cross-reactivity could be due to erythrocyte contamination is ruled out since the cross-reactivity seen in these membranes is equivalent to that seen in a 10-fold dilution of red cell ghost membranes (see lane 1). If this cross-reactivity was due solely to red cell contamination, then the brain membranes would have to contain a 10% contamination with red cells. This is clearly not the case since immunoblot analysis with antibody specific for red cell band 3 indicates that red cell contamination accounts for less than 0.1% of the total brain membrane protein (not shown).

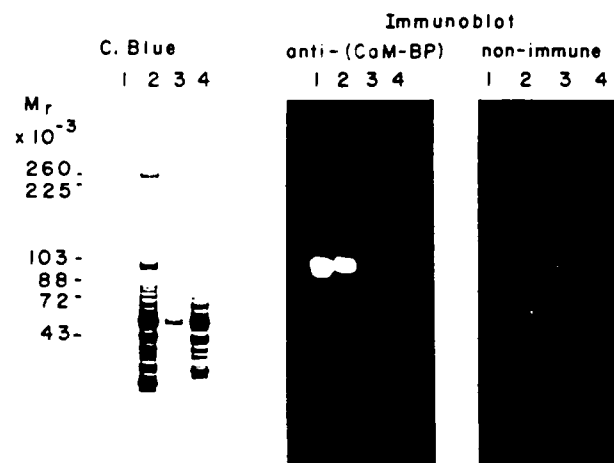


FIG. 10. Identification of a $M_r = 100,000$ peptide(s) in brain that cross-reacts with erythrocyte CaM-BP_{103/97}. Bovine brain was homogenized in 0.25 M sucrose, 7.5 mM sodium phosphate, 100 μ g/ml PMSF, pH 7.5, centrifuged for 5 min at $1,000 \times g$ to remove nuclei and cellular debris. The $1,000 \times g$ supernatant was centrifuged 30 min at $30,000 \times g$ to yield a crude brain membrane pellet and the $30,000 \times g$ supernatant was spun 45 min at $10,000 \times g$ to yield a vesicle pellet. Gel samples from the fractionation steps were processed by electrophoresis on SDS-polyacrylamide exponential gradient gel and stained with Coomassie Blue. Parallel lanes were transferred electrophoretically to nitrocellulose and analyzed by the immunoblot procedure with affinity-purified anti-CaM-BP_{103/97} IgG or affinity-purified nonimmune IgG (see "Experimental Procedures"); erythrocyte ghost membranes (lane 1); 20,000 $\times g$ brain membrane pellet (lane 2); 100,000 $\times g$ brain vesicle pellet (lane 3); 100,000 $\times g$ supernatant (lane 4).

DISCUSSION

This report describes the identification, purification, and characterization of a new calmodulin-binding protein from human erythrocyte membranes. The protein is tightly associated with the membrane skeleton, binds calmodulin with a K_d of 230 nM, and is present at an estimated 30,000 copies/cell. This calmodulin-binding protein (CaM-BP_{103/97}) is a heterodimer with subunits of $M_r = 103,000$ and 97,000 (termed α and β , respectively). Its large frictional ratio (f/f_0) indicates that the protein possesses a high degree of asymmetry. Photoaffinity labeling of the $M_r = 97,000$ β subunit of CaM-BP_{103/97} indicates that the calmodulin-binding site may reside on that polypeptide. Electron microscopic visualization of CaM-BP_{103/97} (Fig. 9) demonstrates that it is a flattened circular molecule with an axial ratio of 2.3. This shape is very similar to that of an oblate ellipsoid of revolution and is consistent with the degree of asymmetry predicted by its hydrodynamically determined frictional ratio. Finally, analogues of CaM-BP_{103/97} may exist in more complex cells since a $M_r = 100,000$ polypeptide(s) has been identified in brain that cross-reacts strongly with affinity-purified anti-CaM-BP_{103/97} IgG and binds calmodulin (Fig. 10).

CaM-BP_{103/97} is not one of the major red cell proteins nor is it a degradation product of these proteins. Therefore, as a protein that represents less than 1% of the total red cell membrane protein, it is not surprising that CaM-BP_{103/97} has gone unnoticed until now. In fact, there are several aspects of CaM-BP_{103/97} and its calmodulin binding activity that may have allowed it to elude recognition over the past few years. First of all, its $M_r = 103,000$ and 97,000 subunits migrate at a position on SDS-polyacrylamide gels that is obscured by band 3 (see Fig. 1). Second, due to the sensitivity of CaM-BP_{103/97} to both degradation by endogenous proteases and cross-linking of its internal sulfhydryl groups (see Figs. 2 and 3), the appearance of these polypeptides on Coomassie Blue-stained gels can be greatly diminished in preparations of membranes where care was not taken to minimize the effects of proteolysis and oxidation.

A third aspect of CaM-BP_{103/97} that may explain why it has evaded detection for so long is its affinity for calmodulin. CaM-BP_{103/97} has a binding constant of 230 nM for calmodulin, which is comparable to the affinity expressed by other calmodulin-binding proteins such as myosin light chain kinase (Johnson *et al.*, 1981), and is physiologically significant since calmodulin is present at micromolar concentrations in the erythrocyte (Jarrett and Penniston, 1978). Nonetheless, the binding of CaM-BP_{103/97} to calmodulin is undetectable in assays of the binding of radiolabeled calmodulin to ghost membranes (Niggli *et al.*, 1979; Agre *et al.*, 1983). This is because the binding by CaM-BP_{103/97} is overwhelmed by the high affinity binding of the $(Ca^{2+} + Mg^{2+})$ -ATPase and other calmodulin-binding proteins of the erythrocyte membrane, which have a K_d for calmodulin in the range of 0.5–75 nM (Agre *et al.*, 1983). It should be pointed out, however, that Scatchard plot analysis of the calmodulin-binding proteins present in the low salt extract of ghost membranes (Agre *et al.*, 1983) indicates binding activities as low as 530 nM.

The formation of an irreversibly cross-linked CaM-BP_{103/97} complex by the ^{125}I -azidocalmodulin photoaffinity label (Fig. 7) is a useful technique for the qualitative detection of calmodulin binding. This technique unfortunately suffers from two major drawbacks in its direct application as a quantitative binding assay. First, a preparation of ^{125}I -azidocalmodulin contains four different species of calmodulin: CaM that is

modified with both the photoactivatable reagent and the Bolton Hunter radiolabel, CaM that is modified with either of the two reagents, and native CaM that is not modified by either reagent. The relative amounts of these species vary among preparations. In view of this, there is no way to obtain a reliable estimate of the true specific activity of the active species, namely the double-modified ^{125}I -azidocalmodulin. This precludes the possibility of obtaining estimates of binding stoichiometries. Second, each of the modifying reagents are amino reactive and highly specific for the lysine residues on calmodulin. Walsh and Stevens (1977) have shown that modification of between 1 and 2 residues of lysine on calmodulin results in 60–70% reduction in its ability to activate its target proteins.

Since the use of ^{125}I -azidocalmodulin alone would produce quantitative errors due to the uncertainty in the specific activity and affinity, we opted to use a competitive assay in which the competing species would be unmodified calmodulin (Fig. 8). The use of this displacement assay in combination with Dixon analysis obviates the need to know the specific activity or affinity of the modified ^{125}I -azidocalmodulin, provided that the two displaced concentrations share the same specific activity. In fact, the analysis outlined by Dixon (1953) describes a method to estimate the affinity of the "substrate" or the competed ^{125}I -azidocalmodulin from the x -intercepts of the Dixon plot (Fig. 8, *inset*). By this method, it is estimated that the ^{125}I -azidocalmodulin used in this study binds CaM-BP_{103/97} with an apparent affinity of 550 nM. This is quite consistent with the 60–70% reduction in affinity that is to be expected by the dual modification of calmodulin.

Hinds and Andreasen (1981) have used an ^{125}I -azidocalmodulin photoaffinity label to detect calmodulin-binding proteins on ghost membranes. The major protein that was labeled in this study was the $(Ca^{2+} + Mg^{2+})$ -ATPase. The lack of labeling of other proteins could be due to the fact that membranes were washed twice prior to photoactivating the label by UV irradiation. This procedure may have dissociated any label bound to CaM-BP_{103/97}. The photoaffinity label, employed in this current study, has been used to label ghost membranes and, if photoactivated before the membranes are washed to remove unbound CaM, a $M_r = 113,000$ radiolabeled complex is formed in these preparations (data not shown). Nonetheless, the $M_r = 113,000$ complex accounts for less than 10% of the total label incorporated into the membrane while the majority of the labeling occurs on the ATPase. This low level of labeling on intact ghost membranes could be due to unfavorable orientations of the photoactivatable groups during photolabeling *in situ* or to the lower affinity of modified calmodulin as described above.

The frictional ratio calculated by the molecular dimensions of CaM-BP_{103/97} estimated by electron microscopy differs by 21% from that determined hydrodynamically (see Tables II and IV). Part of this difference can be accounted for by the differential weight that each calculation places on hydration. Still, there is a large part of this difference that cannot be accounted for entirely by hydration. Thus, CaM-BP_{103/97} is similar to but does not exactly fit the model of an oblate ellipse of revolution. There may be some structural features of CaM-BP_{103/97}, such as a short projection or "tail," that are not accounted for in the model of a rigid ellipsoid of revolution. In support of this, there are several negatively stained images of CaM-BP_{103/97} (Fig. 9, column A), with small irregular projections. Such projections would contribute little to the molecular volume or mass but would have a measurable effect on the frictional ratio.

At the moment, the function of CaM-BP_{103/97} in the red cell or of its analogue in brain is unknown. Many of the known calmodulin-activated proteins have protein kinase or phosphatase activity. Preliminary assays of the purified protein in the absence and presence of Ca²⁺ and calmodulin have revealed no kinase or phosphatase activity toward proteins in intact ghost membranes, cytosol, purified red cell ankyrin, or spectrin. The 110-kilodalton actin-binding protein of the intestinal microvillus (Howe and Mooseker, 1983) shows a superficial resemblance to CaM-BP_{103/97}, but this protein seems linear by electron microscopy and binds calmodulin very tightly in the absence of calcium and thus is distinct from CaM-BP_{103/97}. Although an enzymatic role for CaM-BP_{103/97} cannot be ruled out, the protein may be playing a calcium/calmodulin-regulated structural role in the membrane skeleton. In fact, there are several structural proteins that have calmodulin binding activity. These include spectrin (Sobue *et al.*, 1981a; Berglund *et al.*, 1984), tubulin (Kumagai *et al.*, 1982), caldesmon (Sobue *et al.*, 1981b; Bretscher, 1984), and several of the calmodulin binding "flip-flop" proteins that show calcium/calmodulin-dependent binding to actin filaments (Sobue *et al.*, 1983). Whether or not CaM-BP_{103/97} is related to these flip-flop proteins will require further study.

Since CaM-BP_{103/97} is in the low salt extracts of erythrocytes and is therefore a likely contaminant in crude preparations of spectrin-4.1-actin complexes, its presence along with a small amount of calmodulin remaining from the cytosol could explain the reports of calcium regulation of spectrin-4.1 cross-linking of actin filaments (Fowler and Taylor, 1980). It is particularly interesting in this regard that the number of copies of CaM-BP_{103/97}/cell is very similar to the amount of actin protofilaments/erythrocyte. CaM-BP_{103/97} could be playing a calcium/calmodulin-dependent role in capping or regulating protein association of the actin filaments of the membrane skeleton. The presence of bands that co-migrate with actin and the actin-bundling protein, band 4.9, in the crude preparation of CaM-BP_{103/97} isolated by both DEAE- and CaM-Sepharose affinity chromatography (Figs. 1 and 6) supports this notion. In any case, further characterization of CaM-BP_{103/97} will necessitate the use of reconstitution studies with inside-out vesicles, cytoskeletons, and isolated spectrin-actin complexes in order to determine the true function and mode of regulation of this new protein.

Acknowledgments—We thank Dr. Ueli Aebi for providing the negatively stained micrographs of CaM-BP_{103/97} and for his instructive discussions on protein morphology. We would also like to thank Dr. Pamela Talalay for helpful suggestions during the preparation of the manuscript. We also thank Arlene Daniel, who typed the manuscript.

REFERENCES

- Aebi, U., Fowler, W. E., Isenberg, G., Pollard, T. D., and Smith, P. R. (1981) *J. Cell Biol.* **91**, 340-351.
- Agre, P., Gardner, K., and Bennett, V. (1983) *J. Biol. Chem.* **258**, 6258-6265.
- Andreasen, T. J., Kelier, C. H., LaPorte, D. C., Edelman, A. M., and Storm, O. R. (1981) *Proc. Natl. Acad. Sci. U. S. A.* **78**, 2782-2785.
- Baines, A. J., and Bennett, V. (1985) *Nature* **315**, 410-413.
- Bennett, V. (1983) *Methods Enzymol.* **96**, 313-324.
- Bennett, V. (1985) *Annu. Rev. Biochem.* **54**, 273-304.
- Bennett, V., and Davis, J. (1981) *Proc. Natl. Acad. Sci. U. S. A.* **78**, 7550-7554.
- Bennett, V., and Davis, J. (1982) *Cold Spring Harbor Symp. Quant. Biol.* **46**, 647-657.
- Bennett, V., and Stenbuck, P. J. (1980) *J. Biol. Chem.* **255**, 2540-2548.
- Bennett, V., Davis, J., and Fowler, W. (1982) *Nature* **299**, 126-131.
- Berglund, A., Backman, L., and Shanbhag, V. P. (1984) *FEBS Lett.* **172**, 109-112.
- Bolton, A. E., and Hunter, W. M. (1973) *Biochem. J.* **133**, 529-533.
- Bovam, A. (1968) *Scand. J. Clin. Lab. Invest.* **97**, Suppl. 21, 77-89.
- Bradford, M. M. (1976) *Anal. Biochem.* **72**, 248-254.
- Bretscher, A. (1984) *J. Biol. Chem.* **259**, 12873-12880.
- Cantor, R. C., and Schimmel, P. R. (1980) *Biophysical Chemistry, Part II*, pp. 500-655. W. H. Freeman, San Francisco.
- Cheung, W. Y. (1980) *Science* **207**, 19-27.
- Cohen, C. M. (1983) *Semin. Hematol.* **20**, 141-158.
- Cohen, C. M., and Longley, W. (1966) *Science* **152**, 794.
- Cohen, C. M., Foley, S. F., and Korsgren, C. (1982) *Nature* **299**, 648-650.
- Cohn, E. J., and Edsall, J. T. (1943) *Proteins, Amino Acids, and Peptides*, pp. 370-381. Hainer Publishing Co., Inc., New York.
- Davis, J., and Bennett, V. (1982) *J. Biol. Chem.* **257**, 5816-5820.
- Davis, J., and Bennett, V. (1983) *J. Biol. Chem.* **258**, 7757-7766.
- Davis, J. Q., and Bennett, V. (1984) *J. Biol. Chem.* **259**, 13550-13559.
- Dixon, M. (1953) *Biochem. J.* **55**, 170-171.
- Duong, L. T., Fleming, P. J., and Ornberg, R. L. (1985) *J. Biol. Chem.* **260**, 2393-2398.
- Fairbanks, G., Steck, T., and Wallach, D. (1971) *Biochemistry* **10**, 2606-2617.
- Fischbach, F. A., and Anderegg, J. W. (1965) *J. Mol. Biol.* **14**, 458-473.
- Fowler, V. M., and Bennett, V. (1984) *J. Biol. Chem.* **259**, 5978-5989.
- Fowler, V., and Taylor, D. L. (1980) *J. Cell Biol.* **85**, 361-376.
- Fowler, V. M., Davis, J. Q., and Bennett, V. (1985) *J. Cell Biol.* **100**, 47-55.
- Gietzen, K., and Koldadt, J. (1982) *Biochem. J.* **207**, 155-159.
- Glennay, J. R., Jr., Glennay, P., Osborn, M., and Weber, K. (1982a) *Cell* **28**, 843-854.
- Glennay, J. R., Jr., Glennay, P., and Weber, K. (1982b) *J. Biol. Chem.* **257**, 9781-9787.
- Goewert, R. R., Landt, M., and McDonald, J. M. (1982) *Biochemistry* **21**, 5310-5315.
- Goodman, S. R., and Shiffer, K. (1983) *Am. J. Physiol.* **244**, 121-146.
- Goodman, S. R., Casoria, L., Coleman, D., and Zagon, I. S. (1984) *Science* **224**, 1433-1435.
- Gopalakrishna, R., and Anderson, W. (1982) *Biochem. Biophys. Res. Commun.* **104**, 830-836.
- Granger, B. L., and Lazarides, E. (1984) *Cell* **37**, 595-607.
- Hinds, T. R., and Andreasen, T. J. (1981) *J. Biol. Chem.* **256**, 7877-7882.
- Howe, C. L., and Mooseker, M. S. (1983) *J. Cell Biol.* **97**, 974-985.
- Hunter, W., and Greenwood, F. (1962) *Nature* **194**, 495-496.
- Jarrett, H. W., and Penniston, J. T. (1978) *J. Biol. Chem.* **253**, 4676-4682.
- Johnson, J. D., Holroyde, M. J., Crouch, T. H., Solaro, R. J., and Potter, J. D. (1981) *J. Biol. Chem.* **256**, 12194-12198.
- Kumagai, H., Nishida, E., and Sakai, H. (1982) *J. Biochem. (Tokyo)* **91**, 1329-1336.
- Kuntz, I. D., and Kauzmann, W. (1974) *Adv. Protein Chem.* **28**, 239-345.
- Laemmli, U. K. (1970) *Nature* **227**, 680-685.
- Laurent, T. C., and Killander, J. (1964) *J. Chromatogr.* **14**, 317-330.
- Linder, M. C., Nagel, G. M., Roboz, M., and Hungertford, D. M. (1981) *J. Biol. Chem.* **256**, 9104-9110.
- Lowry, O. H., Rosebrough, N. J., Farr, A. L., and Randall, R. J. (1951) *J. Biol. Chem.* **193**, 265-275.
- Martin, R. G., and Ames, B. N. (1961) *J. Biol. Chem.* **236**, 1372-1379.
- Murakami, T., Hatanaka, M., and Murachi, T. (1981) *J. Biochem. (Tokyo)* **80**, 1809-1816.
- Niggli, V., Ronner, P., Carafoli, E., and Penniston, J. (1979) *Arch. Biochem. Biophys.* **198**, 124-130.
- Quist, E. (1980) *Biochem. Biophys. Res. Commun.* **92**, 631-637.
- Scheraga, H. A. (1961) *Protein Structure*, pp. 1-12. Academic Press, New York.
- Sheetz, M. P., and Singer, S. J. (1977) *J. Cell Biol.* **73**, 638-646.
- Shotton, D. M., Burke, B. E., and Branton, D. (1979) *J. Mol. Biol.* **131**, 303-329.
- Siegel, D. L., and Branton, D. (1985) *J. Cell Biol.* **100**, 775-785.
- Siegel, L. M., and Monty, K. J. (1966) *Biochim. Biophys. Acta* **112**, 346-362.
- Sobue, K., Muramoto, Y., Fujita, M., and Kakiuchi, S. (1981a) *Biochem. Biophys. Res. Commun.* **100**, 1063-1070.
- Sobue, K., Muramoto, Y., Fujita, M., and Kakiuchi, S. (1981b) *Proc. Natl. Acad. Sci. U. S. A.* **78**, 5652-5655.
- Sobue, K., Kanda, K., Adachi, J., and Kakiuchi, S. (1983) *Proc. Natl. Acad. Sci. U. S. A.* **80**, 6868-6871.
- Steck, T. L. (1974) *J. Cell Biol.* **62**, 1-19.
- Tanford, C. (1961) *Physical Chemistry of Macromolecules*, pp. 364-396. John Wiley & Sons, New York.
- Walsh, M., and Stevens, F. C. (1977) *Biochemistry* **16**, 2742-2749.
- Wang, K., and Richards, F. M. (1974) *J. Biol. Chem.* **249**, 8005-8018.
- Weed, R., LaCelle, P., and Merrill, E. (1969) *J. Clin. Invest.* **48**, 795-809.
- Yamamoto, K., and Marchesi, V. T. (1984) *Biochim. Biophys. Acta* **790**, 208-218.
- Yu, J., Fischman, D. A., and Steck, T. L. (1973) *J. Supramol. Struct.* **1**, 233-248.